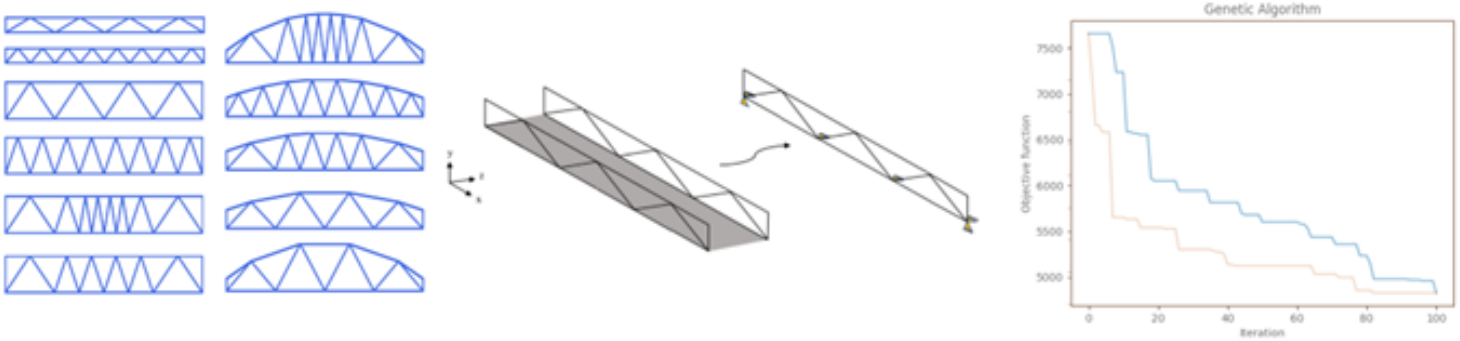

Optimization of Steel Truss Girders in Pedestrian Bridges

Using Genetic Algorithm

Master's thesis in Structural Engineering and Building Technology

EMIL JONBACK
GABRIEL YAKOUB

DEPARTMENT OF ARCHITECTURE AND CIVIL ENGINEERING
DIVISION OF STRUCTURAL ENGINEERING

CHALMERS UNIVERSITY OF TECHNOLOGY
Gothenburg, Sweden 2022 www.chalmers.se

Master's thesis ACEX30

Optimization of Steel Truss Girders in Pedestrian Bridges

Using Genetic Algorithm

EMIL JONBACK
GABRIEL YAKOUB

CHALMERS
UNIVERSITY OF TECHNOLOGY

Department of Architecture and Civil Engineering
Division of Structural Engineering
Lightweight Structures Group
Chalmers University of Technology
Gothenburg, Sweden 2022

Optimization of Steel Truss Girders in Pedestrian Bridges
Using Genetic Algorithm

EMIL JONBACK
GABRIEL YAKOUB

Supervisor: Peter Nilsson Strand, Structural Engineer-Bridges at WSP
Examiner: Mohammad al-Emrani, Full Professor Architecture and Civil Engineering, Structural Engineering, Lightweight Structures

Department of Architecture and Civil Engineering
Division of Structural Engineering
Lightweight Structures Group
Chalmers University of Technology
SE-412 96 Gothenburg
Telephone +46 31 772 1000

Cover: Different topologies for Steel Truss Girders.

Department of Architecture and Civil Engineering
Gothenburg, Sweden 2022

Optimization of Steel Truss Girders in Pedestrian Bridges
Using Genetic Algorithm
EMIL JONBACK
GABRIEL YAKOUB
Department of Architecture and Civil Engineering
Chalmers University of Technology

Abstract

The optimization of any structure is an iterative process, where the Structural Engineer evaluates how certain changes in one or more design variables affect the outcome of the design. With increased number of variables, the design space increases exponentially and it is not feasible to remodel the structure each time and analyze these combinations to choose the best solutions. One way to overcome this problem is by parametric design, where the structure is programmed and governed by a number of parameters so that any change in these parameters would result in a change in this structure. Although this approach saves time when it comes to the modeling process, the designer still needs to run the analysis each time and document the results to select the best set of parameters that fulfills the goals of the design. To overcome this limitation, the implementation of genetic algorithms allow for a faster exploration in the design space to find the most optimal solution.

In this thesis, the steel truss-girders used in single-span pedestrian bridges are studied. A parametric design model is developed to automatically produce these trusses based on a set of parameters that govern the topology of the truss. Furthermore, a finite element analysis is conducted and the necessary design according to Eurocode and the regulations of the Swedish Traffic Administration is done. Finally, a genetic algorithm optimization tool is used to minimize the weight of the truss while fulfilling all the checks.

The study indicates that truss toplogies with bent upper chord have lower weights and this weight difference is increasing with longer spans. Furthermore, it is seen that the diagonals and the upper chord stands for about 70% of the total weight of the truss and yet not fully utilized due to their contribution for the capacity against global buckling which is the most critical check in the design. In addition, using higher steel grade resulted in lighter trusses. However, this effect decreased with longer spans. Global buckling is more critical for trusses with higher steel grades, because the members are only available in cold-formed cross-sections.

Keywords: Steel truss pedestrian bridge, Parametric design, Genetic algorithm, Python, Truss optimization, Topology Optimization.

Acknowledgements

This work has been done in collaboration with WSP in Gothenburg and Chalmers University of Technology.

We would like to express our graditute and give a thank to our supervisor Peter Nilsson from WSP and our examinator Mohammad Al-Emrani from Chalmers for their support and help during all the stages of this work.

Emil Jonback & Gabriel Yakoub , Gothenburg, June 2022

Contents

List of Figures

List of Tables

1
Introduction

1.1 Background

Building and construction industry stands for about 36% of the global energy-related CO2 emissions (UN, 2021). The structure itself in a building stands for more than half of the embodied impact (Kaethner and Burridge, 2012). In Sweden, the building sector stands for about 21% of the emissions (Boverket, 2021). To reach Sweden's goal of net zero emissions by 2045 and in order to minimize these environmental impacts, structural engineers need to be more considerate in their decisions when designing structures.

In today's best practice, the design of steel truss girders used in pedestrian bridges is typically carried out with an initial design that is evaluated against Eurocode. The most common truss type used in these bridges is Warren truss. These trusses are analyzed and based on the utilization ratio some parameters may be changed to reach a higher utilization of the material. Parameters that are normally changed are cross-section variables, while topology is often decided in the preliminary design phase. Cross-section optimization is an undemanding task and it made a small difference when it comes to the resources used in a project when compared to design decisions made in earlier stages, such as topology (Baldock, 2007). By optimizing both the cross-sections and the topology with today's advanced computational power, structural engineers can explore a wider range of design alternatives and choose a structure where the material usage can be minimized. This will lead to both economic benefits as well as environmental benefits, contributing to the goal of reaching net-zero carbon emissions in the Swedish construction industry.

Genetic algorithms (GA) are one good way to optimize a large search space, thanks to its parallel exploration of possible solutions. With the nature-inspired behavior of the algorithm, with concepts such as reproduction, mutation, and survival of the fittest, the potential to optimize trusses is significant. Just as evolution over the span of hundreds of millions of years has evolved the species that inhabit the earth, a genetic algorithm can find an optimized solution to a problem in just hours or days. Implementing GA in the design processes of truss girders used in pedestrian bridges may give a lot of possibilities in optimizing these structures.

1.2 Aim

The aim of this thesis is to study the behavior of steel truss pedestrian bridges that are subject to optimization and how the behavior changes when allowing different design aspects in the bridge.

1.3 Objectives

- Perform a literature study to understand the subject.
- Build a parametric design program that generates a truss-girder and perform a finite element analysis to it.
- Perform the required checks needed to the truss and its members.
- Evaluate how certain parameters affect the weight and behavior of the bridge.

1.4 Limitations

This thesis will not cover the design of the connections between the elements in the truss. However, the angles between the members are restricted to fulfill the requirements. Hot-rolled rectangular & square hollow core sections are the only profiles that will be considered in the thesis. Finally, only single-span pedestrian bridges are studied in this thesis.

1.5 Method

The work in this thesis is performed in the following steps:

- A pre-study is performed, covering the design of truss girders, parametric design and genetic algorithms. This is done through reading publications within the field and collecting and comparing data from current bridges.
- Creation of a parametric design program creating and evaluating trusses. The program is written in Python with help of the CALFEM finite element toolbox.
- Verifying the model and the simplifications done by comparing the results with a commercial finite element software.
- Defining the problem to be optimized and what the goals for the optimization are.
- Connecting the parametric desing program to a genetic algorithm in Python.
- Doing comparisons to evaluate how certain variables in the bridge affect the optimized results.

2

Steel Truss Pedestrian Bridges

A fallen tree across a small river was probably the inspiration for the ancient bridge-builders in history. The first bridges date back to the pre-roman era, in Great Britain for example, a bridge dating back to 3806 B.C. was discovered in Somerset Levels. After developing stone arch building techniques in the Roman era, building construction increased. During the middle-ages and the renaissance, the materials used in bridge construction were stone, masonry and wood. After the industrial revolution, cast iron was used for the first time in bridge construction (Pipinato, 2021). The use of trusses in bridges dates to the 18^{th} century, despite being designed in the 15th and 16th century, by Leonardo da Vinci and Andrea Palladio. Wood was used for the first truss bridges in that period because at that time wooden rods and joints were easy to produce (Andreas, 2013).

Trusses' ability to convert applied loads to tension and compression vectors has made their material efficiency hard to be beaten by other structural solutions. In theory this makes all the truss members take the load axially through bar action, which means that the whole cross-section is active to resist the load (Whitehead, 2019). However, in reality the truss's members are not resisting only axial forces, but shear and bending as well through beam action, however relatively small in comparison to the axial force but they may be crucial in the design. Having members in compression adds a constraint on the length of the members to reduce the risk of buckling. When it comes to members in tension the constraint is that the connections should be able to resist these induced stresses. However, the economical aspect of trusses is not only connected to the material used in its members, but to the fabrication and constructability. Whitehead, 2019 states that faster fabrication diminishes the economic benefits of using various cross-section to save material costs.

There are many truss types according to their geometrical schemes, that were developed over time, maybe the most common ones are Pratt, Howe and Warren trusses which can be seen in subfigures 2.1a to 2.1c. Pratt trusses were first used in 1844 and are suitable for spans of 9-75m. In 1848 Warren trusses made its first appearance and it can be used for spans of 15-120m. Howe trusses are suitable for the shortest spans among these 3 types as it is best used for spans of 9-45m. Howe trusses were first used in 1840 (Pipinato, 2021).

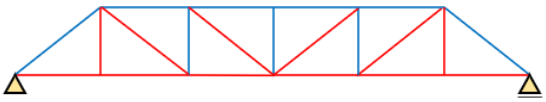

(a) Pratt

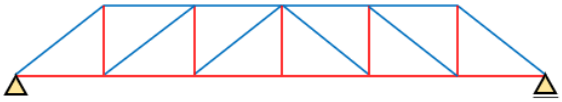

(b) Howe

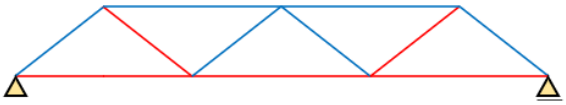

(c) Warren

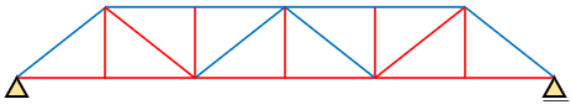

(d) Modified Warren

(e) Vierendeel

Figure 2.1: Types of trusses (Red for members in tension, blue for members in compression

Steel is one of the common materials used in trusses due to its similar strength in tension and compression. However, in compression there is a risk of buckling often leading to a decrease in load capacity. Hollow sections is a material efficient way of increasing the capacity in trusses, due to their high capacity against lateral-torsional buckling, increasing the overall buckling capacity of the truss. (Martin and Purkiss, 2007). Another benefit of using hollow sections over I sections is that the latter one allows dirt and water to accumulate in the joints which affects the bridge's durability (Hirt and Lebet, 2013). If the bridge deck is positioned above the truss, it is called *underspanned system*, if the deck is between the lower and upper chord of the truss it is a *half-through system* and if the deck is below the truss it is a *through system*, see Figure 2.2(Andreas, 2013).

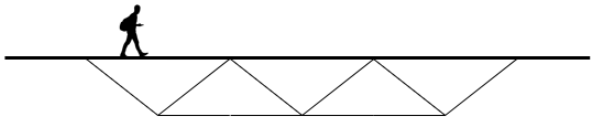

(a) Underspanned System

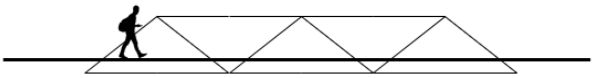

(b) Half-Through System

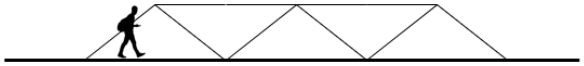

(c) Through System

Figure 2.2: Three types of truss systems

The truss' members are connected in nodes that are called joints. These joints can be formed by either welding the members to each other or by bolting them. A common praxis is to try to make the intersection point of the connected elements axis meet in the same point (Hanses, 2015) . This to prevent getting unwanted induced moments. The most common connections used in steel trusses are illustrated in Figure 2.3. In order to achieve an economical steel structure, it's important to take into consideration the connections when deciding the topology of a truss, because these connections are expensive. (Jaspart and Weynand, 2017).

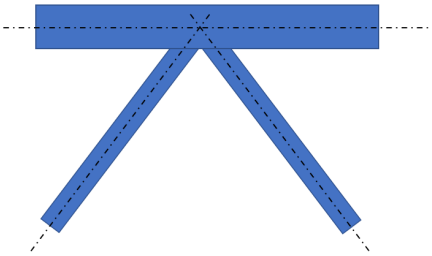

(a) Two welded hollow sections

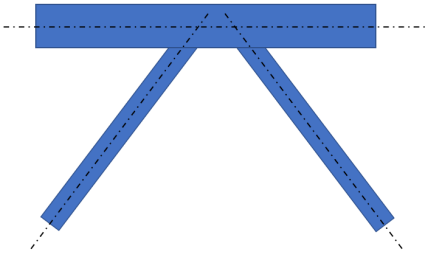

(b) Not centered welded connection

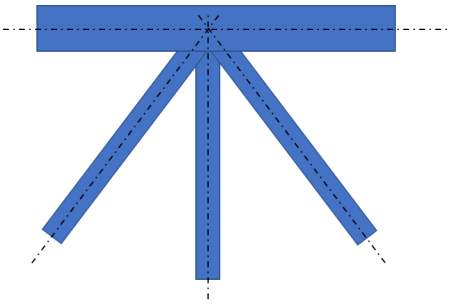

(c) Three welded hollow sections

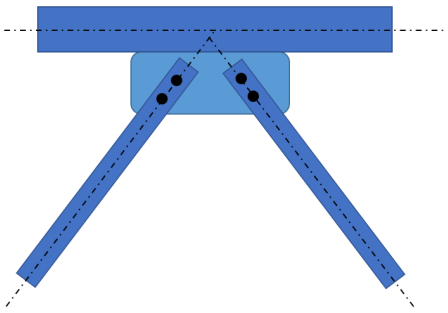

(d) Bolted connection with plate

Figure 2.3: Three types of steel connections

2.1 Today's Best Practice

The information presented in this section is obtained through studying a number of steel truss pedestrian bridges built in Sweden in the past years. The documentations regarding these bridges are collected from The Swedish Traffic Administration's database (BaTMan). The bridges studied are presented in Appendix B

2.1.1 Steel

In Sweden the most common steel quality is S355 and it is used for a majority of the standard profiles delivered by steel manufacturers. The fact that it is the most common steel grade also makes it cheap in comparison to other similar steel grades, because of the larger supply and the cost for factories to convert to producing steel of other grades. In the bridge study it was noted that sometime 20-30 years ago the most common steel grade for steel truss pedestrian bridges changed from S275 to today's S355. Many steel structures are affected by cyclic loads leading to fatigue failure of the steel. However, the fatigue in pedestrian bridges is negligible, due to the small amplitudes of the loads on the bridge. This means that pedestrian bridges could benefit from using higher grade steel. From a pure material perspective, when fatigue is not considered, a higher-grade steel could reduce the material usage in the structure because of its superior strength.

2.1.2 Profiles

Hollow core rectangular profiles are used almost exclusively for steel pedestrian truss bridges in Sweden(BaTMan). One reason that hollow core rectangular profiles are used is that they have a very high torsional resistance(Kabanda and MacDougall, 2017), which eliminates the risk of lateral-torsional buckling. The profiles are either hot-rolled or cold-formed, but mainly hot-rolled profiles are used. Hot rolling steel is a process where the steel is heated up to temperatures around 1000°C and rolled between two cylinders(Soutsos and Domone, n.d.). After the rolling the material is allowed to cool naturally. This process enhances the mechanical properties of the steel and reduces residual stresses. When cold forming steel the steel is treated in temperatures that are below the recrystallisation temperature of the steel. The steel is then drawn through a tapered form, stretching the steel and enhancing the strength. However, this process is affecting the ductility of the material and too much cold forming leads to fracture. There is also higher residual stresses in cold-formed steel compared to hot-rolled steel(Gardner et al., 2010), which is mainly taken into consideration in the design by giving the cold-formed profiles a higher imperfection factor for buckling. In Table 2.1 the type of profile for truss members are put together.

Table 2.1: Profile type for different truss members in bridge study

Truss member	Hot-rolled	Cold-formed
Upper chord	30	6
Lower chord	20	16
Diagonals	19	17

The bridges that have a cold-formed upper chord have cold-formed diagonals and lower chord meaning that there are no bridges combining a cold-formed upper chord with any hot-rolled members. This is due to the fact that the upper chord will be in compression and since cold-formed profiles have a higher imperfection factor for buckling, hot-rolled profiles are favorable for members in compression such as the upper chord. However, cold-formed profiles are cheaper than hot-rolled ones which is the reason for creating trusses that are solely made of cold-formed profiles. For the trusses that have hot-rolled upper chord, one third has cold-formed lower chord and diagonals. Since the lower chord is in tension it is not affected by buckling and the drawback with cold-formed profiles does not matter in that case. Some diagonals will be in compression but not under such high values as the upper chord and the stronger buckling capacity of a hot-rolled profile might not be needed. It can be noted from the table that there is a bridge which has hot-rolled upper and lower chord and cold-formed diagonals. This truss has a significantly larger span than the other trusses in the study, which might explain the unusual combination of profile types.

2.1.3 Topologies

Looking at steel pedestrian truss bridges built in Sweden it is clear that Warren is the most common truss type. In a few cases the truss is a so called Modified Warren, which is basically a Warren truss with verticals, see Figure 2.1d. This is to obtain shorter distance between the joints in the upper chord(Brockenbrough and Merritt, 2016). In the compressed upper chord this may be favorable, since it decreases the local buckling length and gives more lateral support for global buckling. However, the bridges that are studied indicate that Modified Warren is not favorable and that Warren make up a majority of the bridges studied, see Table 2.2. (Figure 2.1e). This could be because the possibility of Modified Warren was not considered in many cases or that Warren was just a better alternative. Vierendeel trusses do not have any inclined diagonals, instead they have only verticals, resulting in a unique behavior

Table 2.2: Truss type for bridges in the bridge study

Modified Warren	7
Pratt	2
Vierendeel	8
Warren	56

Looking at Table 2.3 the weight per square meter does not seem to favor Warren as

much as Table 2.2 would suggest.

Table 2.3: Weight per square meter comparison between Warren and Modified Warren for bridges with similar length and width

Truss type	Length$[m]$	Width$[m]$	Weight$[kg/m^2]$
Modified Warren	27	3.6	34.7
Warren	27.6	3	37.2
Warren	27.5	3	37.6
Warren	27	3.3	42.8

In Table 2.3 the length is the span of the bridge, the width is the distance between the trusses and the weight is total weight divided by length and width. In the study not all the bridges had enough documentation to be able to get the data for Table 2.3 resulting in a quite thin basis to draw conclusions from. But nevertheless the Modified Warren bridge has the lowest weight per square meter and is interesting for future studies.

2.1.4 Production

The production of a steel truss bridge is initiated by the delivery of truss members to the factory where the bridge is to be assembled(Hirt and Lebet, 2013). Long members may be delivered as several shorter parts. Then the bridge is assembled by welding the members in the factory. The welding can be done either manually or automatically. Regardless of the welding technique, the welds need to be inspected to make sure the quality is good. When the welds are inspected and approved the next step is to protect the bridge against corrosion. This is usually done by first sand-blasting the bridge and then coating the bridge with one or several layers of paint. Hot-rolled sections have a layer of iron oxide on the surface, and need to be sand blasted or shot blasted before applying any coating. The blasting is done by applying abrasive particles on the surface with high velocity(Momber, 2008). After painting the bridge it is ready for transportation to the bridge site. Often the pavement is also done in the steel shop before transportation. Transportation can be done either by truck or by boat if the location of the factory and the bridge site is compatible with transportation on water. Pedestrian bridges of this kind usually do not have too long spans, so transportation on roads is a viable option. At the bridge site the bridge is lifted into place with a crane which makes the part of the production that takes place on the bridge site fast and cheap(DeCelle et al., 2013).

2.2 Actions and Loads

When designing a pedestrian bridge various actions and loads need to be considered. The actions that are considered in the design are: self-weight, traffic loads, snow load, wind load & temperature load according to Eurocode SS-EN 1991-2.

2.2.1 Traffic Loads

Traffic loads are divided into a uniformly distributed crowd load with a recommended characteristic value of $q_{fk} = 5kN/m^2$ and a concentrated load $Q_{fwk} = 10kN$. The concentrated load should be applied where it is most critical. However, this concentrated load should not be included if a service vehicle is taken into account, in that case a combination of concentrated loads Q_{serv} acting as shown in Figure 2.4, where $Q_{sv1} = 80kN$ and $Q_{sv2} = 40kN$, is considered instead.

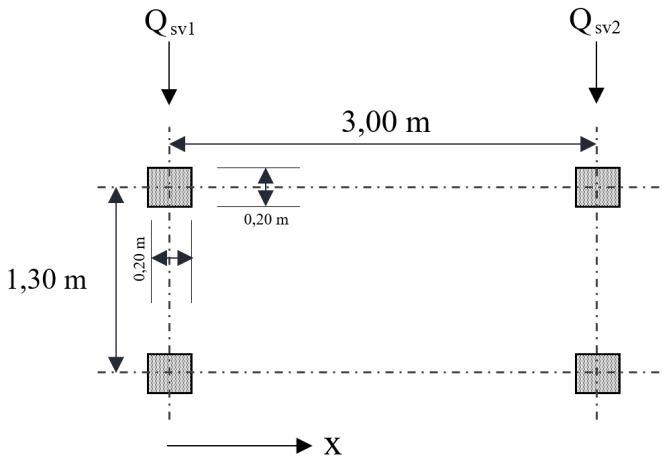

Figure 2.4: Load model for the Service Vehicle

In addition to these vertical loads, a horizontal load Q_{flk} acting along the bridge deck should be included in the design. This load should be taken as the minimum of: 1) 10% of the total uniformly distributed load 2) 60% of the total weight of the service vehicle if it is included. If the concentrated load Q_{fwk} is considered, the horizontal load should not be combined with it. These loads are combined into two groups as shown in Table 2.4.

Table 2.4: Definition of groups of loads (characteristic values)

Load type		**Vertical forces**		**Horizontal forces**
Load systems		Uniformly distributed load	Service vehicle	
Groups of loads	gr1	q_{fk}	0	Q_{flk}
	gr2	0	Q_{serv}	Q_{flk}

2.2.2 Self-Weight

In addition to the self-weight of the members and the deck, the weight of the welds need to be accounted for, according to *TRVK Bro 11*, 2011, this is done by adding an extra $1kN/m^3$. Furthermore, the weight of the railing is added to the total self-weight and it is chosen to $0.16kN/m$. This load is applied on the upper and the lower chord of the truss. A load of $0.13kN/m^2$ is added to account for the pavement, this load is multiplied by the width of the bridge and applied to the lower chord as a line load.

2.2.3 Wind Load

Wind loads acting on a bridge are calculated according to SS-EN 1991-1-4 Section 8. The area that the wind load is applied on is the sum of the areas of the truss elements' face against the wind direction. The load is then applied as a line load on the members. The dynamic response of the bridge due to wind load is not investigated in this thesis because the assumed span is less than 40m. The bridge is assumed to be located in Gothenburg where the basic wind velocity is $v_b = 25m/s$,$\rho = 1.25kg/m^3$, and the terrain category is chosen to type II.

The wind force is calculated according to the expression:

$$F_W = \frac{1}{2}{}_b^2 C A_{ref,x} \tag{2.1}$$

Where the force factor C is obtained from Table 8.2 in SS-EN 1991-1-4 , where $\frac{b}{d_{tot}} = 0.5$ and $z_e \leq 20$. The force factor is then $C = 6.7$.

Two cases should be considered. The first one is wind on a bridge without traffic and the other is on a bridge with traffic. The first case is obtained by calculating the solidity ratio:

$$\phi = \frac{A}{A_c} \tag{2.2}$$

Where A is the sum of the projected area of the members and A_c is the overall envelop area. In the first case $0.3m$ is added according to SS-EN 1991-1-4 to $\phi * H_{truss}$ to obtain the parameter d and then the line load Q_w is obtained by the expression:

$$Q_w = dF_W \tag{2.3}$$

In the second case, where the bridge is considered with traffic, the area is calculated by using $d = 1.5m$ for traffic area and adding the heights of the upper and the lower chords.
This load is then divided between the upper chords, lower chords and diagonals corresponding to their areas which are facing the wind direction using the expression:

$$Q_z = \frac{1}{2} dF_W / L_{part} \tag{2.4}$$

2.2.4 Load Combinations

In this thesis the load combinations will include, in addition to the loads in Table 2.4, the self-weight of the structure (deck & truss) & the wind load acting out-of-plane on the truss. The snow load is not to be combined with load group gr1 & gr2, according to Eurocode and thus not included in this thesis. Temperature loads are also neglected because the structure is simply supported and therefore the temperature will not induce any forces in the structure. In load combination 6.10b the variable load is dominant and this will be the load case that is used.

Table 2.5: Factors for permanent loads

Permanent Loads	**6.10a ULS**		**6.10b ULS**		**6.10ab SLS**	
	max	min	max	min	max	min
γ_G	1.35	1	1.2	1	1	1

Table 2.6: Factors for variable loads

Variable Loads	**6.10a ULS**		**6.10b ULS**		**6.10ab SLS**	
	ψ_0	ψ_0	ψ_0	ψ_0	ψ_1	ψ_2
γ_G	0.6	0.6	1.5	0.6	0.4	0

Table 2.7: Load combinations ULS 6.10a

Load Combination	Self-weight	Traffic Load	Service Vehicle	Wind Load
gr1 - Main	1.35	0.6	0	0.6
gr2 - Main	1.35	0	0.6	0.6
Wind Load - Main	1.35	0.6	0	0.6
Wind Load - Main	1.35	0	0.6	0.6

Table 2.8: Load combinations ULS 6.10b

Load Combination	Self-weight	Traffic Load	Service Vehicle	Wind Load
gr1 - Main	1.2	1.5	0	0.6
gr2 - Main	1.2	0	1.5	0.6
Wind Load - Main	1.2	0.6	0	1.5
Wind Load - Main	1.2	0	0.6	1.5

Table 2.9: Load combinations SLS 6.10ab

Load Combination	Self-weight	Traffic Load	Service Vehicle	Wind Load
Traffic Load - Main	1	0.4	0	0

2.3 Eurocode

The bridge's load-carrying capacity needs to be verified according to Eurocode. To do this the bridge needs to pass certain checks. The formulas and demands presented in this chapter is based on SS-EN 1993-1-1:2005 and SS-EN 1993-2:2006 unless otherwise is stated.

2.3.1 Tension

If the beam is loaded in tension, then the resistance of the cross-section is calculated accordingly

$$N_{t,Rd} = \frac{A \cdot f_y}{\gamma_{M0}} \tag{2.5}$$

Where,

$N_{t,Rd}$ is the tensile capacity of the cross-section $[N]$
A is the cross-sectional area $[mm^2]$
f_y is the steel yield strength $[MPa]$
γ_{M0} is a partial safety factor [-]

2.3.2 Compression

The resistance of a cross-section in compression is dependent of the cross-section class. Class 4 cross-sections are not covered in this work and for all other cross-section classes the resistance is calculated as follows

$$N_{c,Rd} = \frac{A \cdot f_y}{\gamma_{M1}} \tag{2.6}$$

Where,

$N_{c,Rd}$ is the compressive capacity of the cross-section $[N]$
A is the cross-sectional area $[mm^2]$
f_y is the steel yield strength $[MPa]$
γ_{M1} is a partial safety factor [-]

2.3.3 Buckling

If a beam is loaded in compression and there is a risk of buckling a buckling reduction factor χ is introduced. The resistance of the cross-section is then calculated accordingly

$$N_{b,Rd} = \frac{A_y \cdot \chi}{\gamma_{M0}} \tag{2.7}$$

Where,

$N_{b,Rd}$ is the compressive capacity of the cross-section $[N]$
A is the cross-sectional area $[mm^2]$

f_y is the steel yield strength $[MPa]$
χ is the buckling reduction factor [-]
γ_{M0} is a partial safety factor [-]
The buckling reduction factor χ is calculated as

$$\chi = \frac{1}{\Phi + \sqrt{\Phi^2 - \bar{\lambda}^2}} \tag{2.8}$$

Where,

$\Phi = 0,5[1 + \alpha(\bar{\lambda} - 0,2) + \bar{\lambda}^2]$

$\bar{\lambda} = \sqrt{\frac{A \cdot f_y}{N_{cr}}}$

α is an imperfection factor $[-]$

$N_{cr} = \frac{\pi^2 \cdot EI}{L_{cr}^2}$ is the critical buckling force $[N]$

Where L_{cr} is the buckling Length $[m]$

For in plane buckling the buckling length is set to 0,9 times the actual length of the element. For out of plane buckling the buckling length is set as the actual length of the element.

2.3.4 Cross-Section Class

The classification of the cross-section is done according to table 5.2 in SS-EN 1993-1-1:2005.

For rectangular hollow cross-sections:

$$c/t \leq 33\varepsilon^2 \text{ class 1} \tag{2.9}$$

$$c/t \leq 38\varepsilon^2 \text{ class 2} \tag{2.10}$$

$$c/t \leq 42\varepsilon^2 \text{ class 3} \tag{2.11}$$

Where,

$$\varepsilon = \sqrt{235/f_y} \tag{2.12}$$

And,

c is the maximum distance between the edges of the rectangle
t is the cross-sectional thickness
f_y is the steel yield strength $[MPa]$

2.3.5 Shear

The shear capacity of the cross-section is calculated according to section 6.2.6 in SS-EN 1993-1-1:2005.

$$V_{pl,Rd} = \frac{A_v(f_y/\sqrt{3})}{\gamma_{M0}} \tag{2.13}$$

Where A_v is the shear area and should be taken as:

a) $Ab/(b+h)$ for rolled rectangular hollow sections of uniform thickness (Load parallel to width).
b) $Ah/(b+h)$ for rolled rectangular hollow sections of uniform thickness (Load parallel to depth).

Where,

A is the cross-sectional area
b is the overall breadth
h is the overall depth
f_{y} is the steel yield strength $[MPa]$
γ_{M0} is a partial safety factor [-]

2.3.6 Moment

The moment capacity of the cross-section about one principal axis is calculated according to section 6.2.5 in SS-EN 1993-1-1:2005

$$M_{c,Rd} = M_{pl,Rd} = \frac{W_{pl} f_y}{\gamma_{M0}} \text{ for cross-sections in class 1 or 2} \tag{2.14}$$

$$M_{c,Rd} = M_{el,Rd} = \frac{W_{el,min} f_y}{\gamma_{M0}} \text{ for cross-sections in class 3} \tag{2.15}$$

Where,

W_{pl} is the plastic section modulus $[mm^3]$
W_{el} is the elastic section modulus $[mm^3]$
f_{y} is the steel yield strength $[MPa]$
γ_{M0} is a partial safety factor [-]

2.3.7 Tensile Axial Force & Bending

SS-EN 1993-1-1:2005

$$\frac{N_d}{N_{t,Rd}} + \frac{M_{zd}}{M_{z,Rd}} + \frac{M_{yd}}{M_{y,Rd}} \leq 1 \tag{2.16}$$

2.3.8 Axial Compression & Bending

The interaction is calculated according to SS-EN 1993-1-1:2005. The following auxiliary terms are calculated according to table A1 in Annex A.

$$\frac{N_d}{N_{b,Rd}} + k_{yy}\frac{M_{zd}}{M_{z,Rd}} + k_{yy}\frac{M_{yd}}{M_{y,Rd}} \leq 1 \tag{2.17}$$

$$\frac{N_d}{N_{b,Rd}} + k_{zy}\frac{M_{zd}}{M_{z,Rd}} + k_{zz}\frac{M_{yd}}{M_{y,Rd}} \leq 1 \tag{2.18}$$

Where the interaction factors are, for cross-section class 1 and 2:

$$k_{yy} = C_{my}C_{mLT}\frac{\mu_y}{1-\frac{N_{Ed}}{N_{cr,y}}}\frac{1}{C_{yy}} \tag{2.19}$$

$$k_{yz} = C_{mz}\frac{\mu_y}{1-\frac{N_{Ed}}{N_{cr,z}}}\frac{1}{C_{yz}}0.6\sqrt{\frac{w_z}{w_y}} \tag{2.20}$$

$$k_{zy} = C_{my}C_{mLT}\frac{\mu_z}{1-\frac{N_{Ed}}{N_{cr,y}}}\frac{1}{C_{zy}}0.6\sqrt{\frac{w_y}{w_z}} \tag{2.21}$$

$$k_{zz} = C_{mz}\frac{\mu_z}{1-\frac{N_{Ed}}{N_{cr,z}}}\frac{1}{C_{zz}} \tag{2.22}$$

and for cross-section class 3 and 4:

$$k_{yy} = C_{my}C_{mLT}\frac{\mu_y}{1-\frac{N_{Ed}}{N_{cr,y}}} \tag{2.23}$$

$$k_{yz} = C_{mz}\frac{\mu_y}{1-\frac{N_{Ed}}{N_{cr,z}}} \tag{2.24}$$

$$k_{zy} = C_{my}C_{mLT}\frac{\mu_z}{1-\frac{N_{Ed}}{N_{cr,y}}} \tag{2.25}$$

$$k_{zz} = C_{mz}\frac{\mu_z}{1-\frac{N_{Ed}}{N_{cr,z}}} \tag{2.26}$$

Where,

$$C_{yy} = 1 + (w_y - 1)\left[\left(2 - \frac{1.6}{w_y}C_{my}^2\bar{\lambda}_{max} - \frac{1.6}{w_y}C_{my}^2\bar{\lambda}_{max}^2\right)n_{pl} - b_{LT}\right] \geq \frac{W_{el,y}}{W_{pl,y}} \tag{2.27}$$

$$C_{yz} = 1 + (w_z - 1)\left[\left(2 - 14\frac{C_{mz}^2\lambda_{max}^2}{w_z^5}\right)n_{pl} - c_{LT}\right] \geq 0.6\sqrt{\frac{w_z}{w_y}}\frac{W_{el,z}}{W_{pl,z}} \tag{2.28}$$

$$C_{zy} = 1 + (w_y - 1)\left[\left(2 - 14\frac{C_{my}^2\lambda_{max}^2}{w_y^5}\right)n_{pl} - d_{LT}\right] \geq 0.6\sqrt{\frac{w_y}{w_z}}\frac{W_{el,y}}{W_{pl,y}} \tag{2.29}$$

$$C_{zz} = 1 + (w_z - 1)\left[\left(2 - \frac{1.6}{w_z}C_{mz}^2\bar{\lambda}_{max} - \frac{1.6}{w_z}C_{mz}^2\bar{\lambda}_{max}^2\right)n_{pl} - e_{LT}\right] \geq \frac{W_{el,z}}{W_{pl,z}} \quad (2.30)$$

$$\mu_y = \frac{1 - \frac{N_{Ed}}{N_{cr,y}}}{1 - \chi_y \frac{N_{Ed}}{N_{cr,y}}} \quad (2.31)$$

$$\mu_z = \frac{1 - \frac{N_{Ed}}{N_{cr,z}}}{1 - \chi_z \frac{N_{Ed}}{N_{cr,z}}} \quad (2.32)$$

Where,

$$n_{pl} = \frac{N_{Ed}}{N_{Rk}/\gamma_{M1}} \quad (2.33)$$

$$W_y = \frac{W_{pl,y}}{W_{el,y}} \leq 1.5 \quad (2.34)$$

$$W_z = \frac{W_{pl,z}}{W_{el,z}} \leq 1.5 \quad (2.35)$$

Constant moment diagram is assumed ($\Psi_y = \Psi_z = 1.0$) and according to table A2 in Annex A:

$$C_{mi,0} = 0.79 + 0.21\Psi_i + 0.36(\Psi_i - 0.33)\frac{N_{Ed}}{N_{cr,i}} \quad (2.36)$$

Because the considered cross-sections in this thesis are not prone to lateral-torsional buckling, the following terms are predefined:

$$\chi_{LT} = 1.0 \quad (2.37)$$

$$a_{LT} = b_{LT} = c_{LT} = d_{LT} = e_{LT} = 0 \quad (2.38)$$

$$\lambda_0 = 0 \quad (2.39)$$

$$C_{mLT} = 1.0 \quad (2.40)$$

$$C_{my} = C_{my,0} \quad (2.41)$$

$$C_{mz} = C_{mz,0} \quad (2.42)$$

2.3.9 Global Buckling

The compressed upper chord needs to be checked for global buckling. In the global analysis the chord is treated as a column with lateral spring supports based on the diagonals (See Figure 2.5).

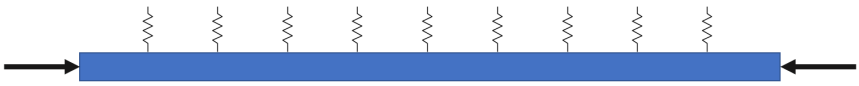

Figure 2.5: The Upper Chord as a Simply Supported Column with Lateral Springs

In each joint where diagonals connect to the upper chord a spring support with stiffness C is modeled. The stiffness C is decided as follows

$$C = \frac{A + B - 2D}{AB - D^2} EI_u \tag{2.43}$$

Where,

$$A = \frac{h^2 I_u}{n_l} + \frac{d_l^3 I_u}{3I_{dl}} + \frac{a^2 u}{3} \tag{2.44}$$

$$B = \frac{h^2 I_u}{n_r} + \frac{d_r^3 I_u}{3I_{dr}} + \frac{b^2 u}{3} \tag{2.45}$$

$$n_l = \frac{2}{b_q} I_{ql} + \frac{GI_{Tl}}{Eu_l} \tag{2.46}$$

$$n_r = \frac{2}{b_q} I_{qr} + \frac{GI_{Tr}}{Eu_r} \tag{2.47}$$

$$D = \frac{1}{6} abu \tag{2.48}$$

Where,
I_{dl}, I_{dr}, I_u is the moment of inertia for out of plane bending for diagonals and lower chords $[mm^4]$
I_{ql}, I_{qr} is the moment of inertia for bending around the longitudinal direction of the bridge for the cross beams $[mm^4]$
GI_{Tl}, GI_{Tr} is the St.Venant torsional stiffness of the adjacent chords $[Nmm^2]$

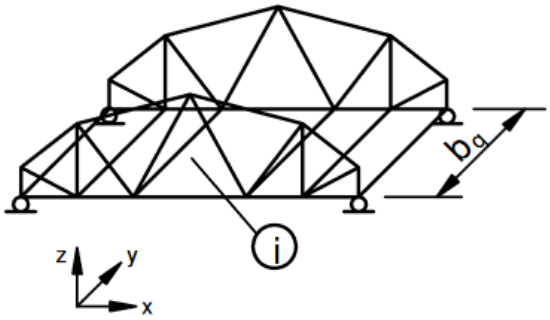

(a) Bridge Model

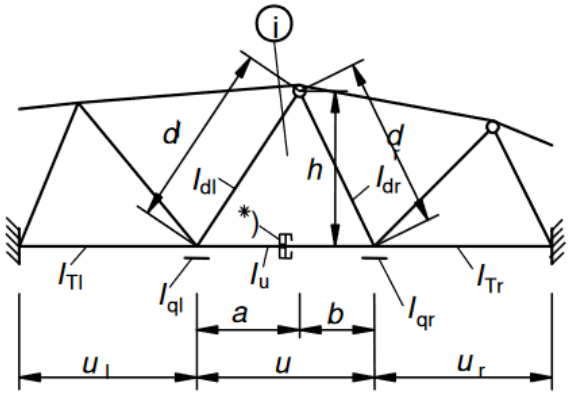

(b) Section for Calculating Spring Stiffness

Figure 2.6: Model for spring stiffness from Eurocode

$$L_{cr} = \frac{\pi}{\sqrt[4]{\frac{4C}{aEI}}} \tag{2.49}$$

Where,
C is the average spring stiffness obtained using equation 2.43$[N/mm]$
a is the average distance between joints in the upper chord $[mm]$

$$\bar{\lambda} = \frac{L_{cr}}{i}\frac{1}{\lambda_1} \tag{2.50}$$

Lambda is then used in the procedure of calculating the compressive capacity of the cross-section as in section 2.3.3

2.3.10 Deflection

The bridge needs to fulfill demands on the vertical deformation. In Sweden the limit for deflection is set by Trafikverket to 1/400 times the span length(*TRVK Bro 11*, 2011). This check should be executed in the serviceability limit state.

3

Parametric Design and Optimization

3.1 Parametric Design

Parametric design is a process that allows designers to define their models by a set of governing parameters (Holzer et al., 2007). Instead of drawing a line, for instance, the designer defines two points that are connected through a line (See Subfigure 3.1a). By changing the coordinates of the point, the line is changed. The same applies to a 3D-cylinder where the parameters that govern the geometry are: the center of the circle, the radius and the height. Other important parameters can be the plane where the geometry is placed. This process is also called computational thinking. The final outcome is broken down into steps that the program will follow to reach the final result (Ajouz, 2007). One example of the early use of parametric design was in Antoni Gaudí's work in Sagrada Família, where he used parametric equations (Makert and Alves, 2016).

(a) Parametric Line **(b)** Parametric Cylinder

Figure 3.1: Parametric Geometries

The implementation of parametric design enables the designer to include optimization in the early design phases and not keep it as a final stage after the structural design is finished (Holzer et al., 2007). This automation opens for possibilities to rapidly evaluate how a change in a set of parameters influences the design and made design decisions, instead of building a new model every time a change needs to be evaluated.

3.2 Optimization in Structural Engineering

One simple example of optimization is to utilize a cross-section as far as possible, to reduce the costs for a client and to reduce the carbon footprint of a structure. In Ching and Carstensen, 2022 it is mentioned that there are two ways of reducing the embodied carbon, either by using materials that has low impact on the environment, or by structural optimization. Mathematically, any optimization problem can be described as finding x, which is a vector containing n components, to minimize the objective function $f(x)$ subjected to m-number of inequality-constraints g and j-number of equality-constraints h. The general mathematical expression for optimization is as follows:

$$\begin{gathered}\text{Minimize } f(x) \\ \text{Subjected to } g_i(x) \geq 0 \\ \text{And } h_j(x) = 0 \\ \text{Where } i = 1, \ldots, m \ \& \ j = 1, \ldots, l\end{gathered}$$

And x is within two defined bounds.

For instance, the optimization of a cantilever steel beam with regard to weight would be to find the minimum cross-section with maximum utilization that fulfills the following conditions – constraints: utilization of the material and the deflections should be under a certain value. So $f(x)$ is a function representing the weight and the constraints $g_{\mathrm{i}}(x)$ are functions that express the utilization and deflection. The constraint functions in this case are created by taking the allowed value of either utilization ratio or deflection, and then subtracting the actual value obtained when analyzing the cantilever steel beam. If the function has a value below zero then the constraints are not fulfilled.

For an optimization problem, Kirsch, 1993 defines a number of design variables that govern the design. These are: material design variables, topological design variables, geometrical design variables and cross-sectional design variables. The number of material design variables for a steel truss is small, the members can be chosen with different yield strengths for instance, in this case Kirsch means that it is more efficient to run an optimization for each yield strength rather than making this variable changeable during the optimization. The other variables are basically what defines the different types of optimization.

Structural optimization can be divided into two categories, geometrical and topology optimization, and geometrical optimization is divided into shape and size optimization.

3.2.1 Size Optimization

Also called cross-sectional optimization. For members of a steel truss, size optimization can be described as finding the most efficient cross-sectional area or moment

of inertia that fulfills the predefined criteria and strength controls (Compare Figures 3.2a and 3.2b). This can be for example the deflection of the truss. For a determinate structure, this can be a straightforward procedure. But for an indeterminate structure, several iterations are required. The reason is that changing the cross-section would change the stiffness of the structure and thus change the load distributions (Debney, 2020). One of the constraints in size optimization that Debney, 2020 highlight, is that the designer is restricted to the cross-sections provided by the manufacturer. Furthermore, thinking of cost efficiency, sometimes choosing a minimum cross-section would require welding stiffeners which is a rather more expensive solution compared to choosing a larger cross-section, and lightweight slender profiles result in an increased risk for buckling.

3.2.2 Shape Optimization

In this type of optimization, for a truss, for instance, the location and the coordinates of the nodes, and the depth of the truss are changed to find the optimal solution (Compare Subfigures 3.2a and 3.2c). The number of elements, the topology and the cross-sections of the elements are not changed (Debney, 2020). These changes in the positions of the nodes will result in changes in the member inclinations and thus reduce or increase the forces in these members, the length of the members will also be changed.

3.2.3 Topology Optimization

While shape optimization allows only the coordinates of the nodes to be changed, topology optimization allows to add and delete members and nodes from an initial ground structure that is similar to a grid, this is called The Ground Structure Approach. This means that with an increased number of joints and members in the initial ground structure, the number of possible node locations would increase. One way to set a limit to this large number of solutions is by specifying the number of allowable joints in the design, but this has a drawback which is that the optimal solution may not be included.

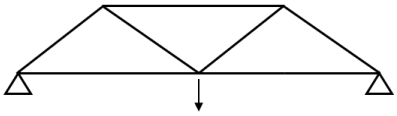

(a) Initial Truss

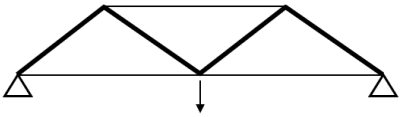

(b) Size Optimized Truss

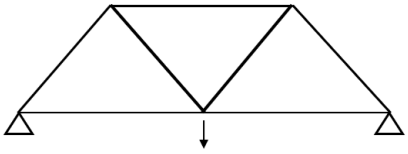

(c) Shape and Size Optimized Truss

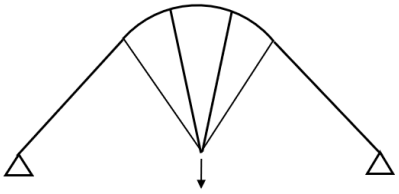

(d) Toplogy, Shape and Size Optimized Truss

Figure 3.2: Types of Optimization

3.2.4 Constraints

To reach a feasible design, the most useful design variables must be chosen. The criteria to evaluate the usefulness of these variables are the constraints. Kirsch, 1993 divides the constraints into two categories, technological constraints and behavior constraints. The first one defines the lower and the upper bound of the design variables. The second one defines the requirements that needs to be fulfilled, like the maximum utilization of the cross-section, maximum stresses, displacement etc.

3.2.5 Type of Optimization

Optimization can be classified into two categories according to its number of objectives, single-objective and multi-objective(multi-criteria). In the latter one, the optimization has two or more objective functions, these functions can for example be to maximize the utilization and minimize the deflections and the cross-sectional area. These objectives can be conflicting. Furthermore, another classification can be regarding the constraint (constrained, unconstrained), the variables (discrete, continuous), function form (linear, non-linear) (Yang, 2010).

3.2.6 Optimization Methods

When it comes to optimization methods, they are divided into two categories, deterministic algorithms, and stochastic algorithms. An example of stochastic algorithms are genetic algorithms, in these types of algorithms the solutions will be different every time the optimization is ran due to the randomness of the stochastic algorithms compared to the deterministic ones where the path toward the solutions is the same every time the optimization is ran assuming the same design variables every run(Yang, 2010).

3.2.7 Drivers for Optimization

Baldock, 2007 introduces the main drivers for optimization in the building industry:

- Financial benefits in term of material savings and reduced construction cost.
- The ability to automate the search of different alternatives saves time and reduces the costs in term of time set on exploring different iterations.
- Increasing the potential of discovering a large number of alternatives in a small amount of time.

3.3 Genetic Algorithms

Genetic algorithms are a type of stochastic evolutionary algorithms, inspired by nature and Darwin's theory of natural selection(Yang, 2014). Through evolutionary phenomena such as reproduction, mutation and survival of the fittest, an optimal individual is generated. Genetic algorithms can handle many different problems, for instance transient and nonlinear problems. The algorithms will, just like nature, explore many different solutions thanks to mutation, which will minimize the probability of finding a local optimum.

3.3.1 Generation

An iteration in the algorithm is called a generation. In each generation there is a population of individuals. The number of generations is set before the algorithm is ran, meaning that there are no convergence issues that will lead to the algorithm not ending. However, this means that premature convergence and local optima may occur without any clear indications. To avoid this, parameters such as population size, mutation and crossover probability, and number of generations should be tested with various values to try and get the solution to converge to a global optimum(Kramer, 2017). Generally genetic algorithms easily discover the global optimum with some tuning of the previously mentioned parameters(Sivanandam and Deepa, 2008), to run the algorithm several times is a way to verify that the optimum is global because of the randomness of stochastic algorithms.

3.3.2 Strings

Each individual is represented by a binary string, consisting of zeros and ones. The numbers in the strings are called alleles, a group of alleles that gives the individual a certain characteristic is called a gene(Rothlauf, 2006). Together the alleles and genes form a chromosome that represents all genetic information of the individual.

3.3.3 Population

The population is consisting of a given number of individuals. Through crossover, mutation, and survival of the fittest the population generates a new population for the next generation. The choice of population size is done before the algorithm is started and may affect the result negatively if too small. A too small population may lead to premature convergence, if an individual with a high fitness value appears early in the algorithm it can, along with its offspring, take over the entire population. If it appears too early the algorithm won't have time to explore enough subspaces before convergence occurs, leading to a local optimum.

3.3.4 Crossover

In the creation of a new generation with a new population, crossover is an important part.

$$\left[\begin{array}{ccccc|ccc} 1 & 0 & 1 & 1 & 0 & 1 & 0 & 1 \\ 0 & 1 & 0 & 1 & 0 & 0 & 1 & 1 \end{array}\right]$$

$$\left[\begin{array}{ccccc:ccc} 1 & 0 & 1 & 1 & 0 & 0 & 1 & 1 \\ 0 & 1 & 0 & 1 & 0 & 1 & 0 & 1 \end{array}\right]$$

Figure 3.3: Parent strings and their offspring

Two individuals from the current population are chosen as parents, and by cutting their gene strings at the same place, they can be combined to get an offspring in the form of two new individuals as seen in figure 3.3. The probability for crossover happening is decided by a parameter p_c. This parameter should have a high value since this is the main evolutionary operator.

3.3.5 Mutation

Constantly reproducing the fittest individuals may lead to premature convergence, because the fittest individuals may be part of a subspace. If the fittest individuals all have a zero in the first bit, then all the new individuals will be in that subspace. By using mutation, the individuals may get out of that subspace and perhaps find a better solution than the ones in the subspace where all individuals have a zero in the first bit(Holland, 1992). The subspace may be more specific than just the first bit being the same for all individuals. If all the individuals have this composition [1**0*1], where the given numbers are the same for all the individuals and * means that the gene can be either 0 or 1, then all those individuals belong to the same subspace of the solution. But through mutation the first gene, which is a 1 for all the individuals, may turn into a 0 and hence explore a new part of the design space. The probability of mutation is just as for crossover decided by a parameter m_c. To avoid that the mutation makes the algorithm randomly search the space of solutions, this parameter should not have a very high value.

3.3.6 Phenotype

The binary strings, or chromosomes, representing each individual need to be translated into structural models. This is done through a so-called phenotype-genotype mapping(Rothlauf, 2006). Here the binary strings will convert to values and coordinates that build up the structural model. For instance, a gene consisting of 6 alleles can take 2^6 or 64 different values. More alleles or bits in a gene will lead to a higher precision in the gene but also require more extensive computing.

3.3.7 Fitness Function

To decide which individuals are more likely to reproduce, a fitness function is stated. The function can consist of several criteria that should be minimized or maximized, but the more parallel criteria the higher the complexity and computational demand.

The individuals will be evaluated against these criteria and be given a fitness value. Individuals with high fitness will move on to the next generation, along with their offspring from crossover. Low fitness individuals will be eliminated for the next generation.

3.3.8 Penalty Function

When the genetic algorithm explores a solution space it will do so without considering any constraints other than the boundaries for the input variables to the fitness function. The genetic algorithm will create trusses without considering all constraints, which may lead to unstable structures or structures that can't be manufactured. To make sure that the algorithm does not converge to this type of solutions, a penalty function is introduced. If an individual breaks against any constraints it will be given a penalty that lowers its fitness value.

4

Structural Model

Trusses ideally carry loads axially, but in reality moments and shear forces affect the truss members. Therefore, 3D beam elements are used in the finite element model instead of bar elements. Each node in the 3D beam element has 6 degrees of freedom, 3 translation (u) in x,y,z direction and 3 rotation (z) around x-,y-,z-axis as seen in Figure 4.1.

Figure 4.1: Degrees of freedom of a 3D beam element

The truss is simply supported and the deck is assumed stiff in z direction, so that the nodes of the elements of the lower chord are modeled as supported in that direction (see Figure 4.2). In addition, only one truss, without composite action with the bridge deck, is studied in this thesis, and thus the loads described in Section 2.2 are divided equally and applied on the truss.

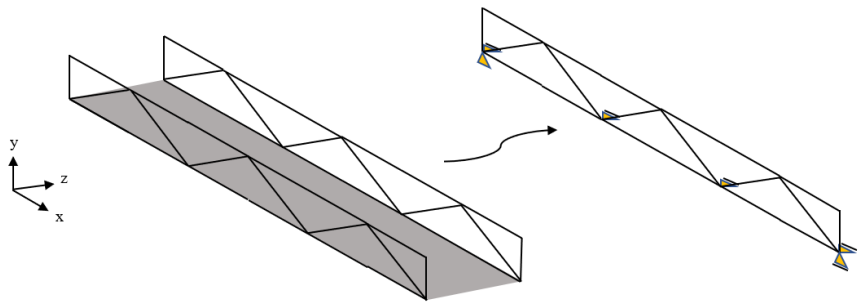

Figure 4.2: The structural model approximation of a steel-truss pedestrian bridge

In CALFEM, the self-weight of the elements can not be included implicitly in the analysis and loads can only be applied in the direction of the elements coordinates system, which means that any gravity load of inclined members can not be included in the analysis. To overcome this limitation in CALFEM, the gravity load of each member is applied by dividing it into its two components, the first one is applied axially on the member in the direction of the member's local x-axis, while the second one is applied as a uniform distributed load in the opposite direction of the member's local y axis as shown in Figure 4.3.

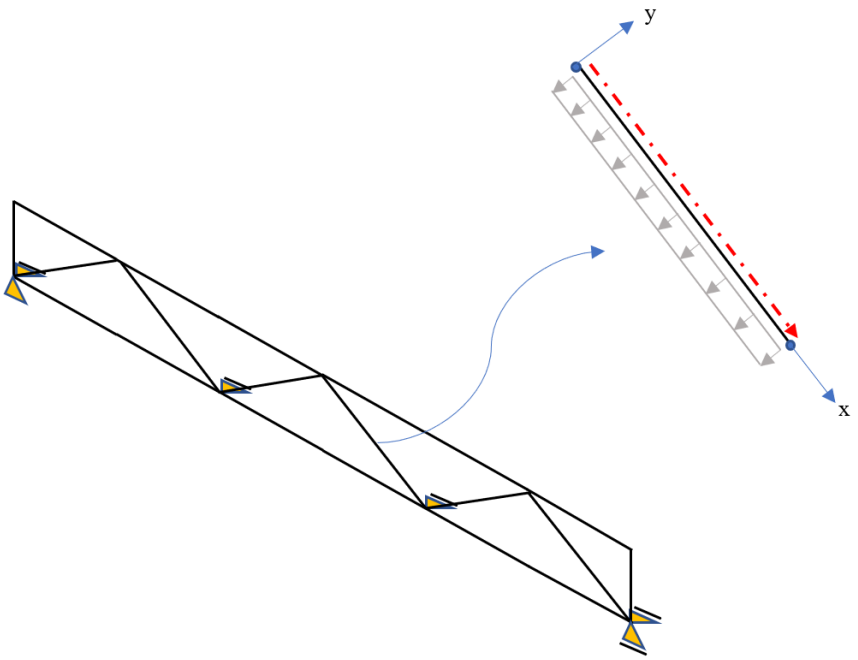

Figure 4.3: The self-weight of a truss member

The wind load is applied in the direction of the member's z-axis which coincide with

the global z-axis as shown in Figure 4.4.

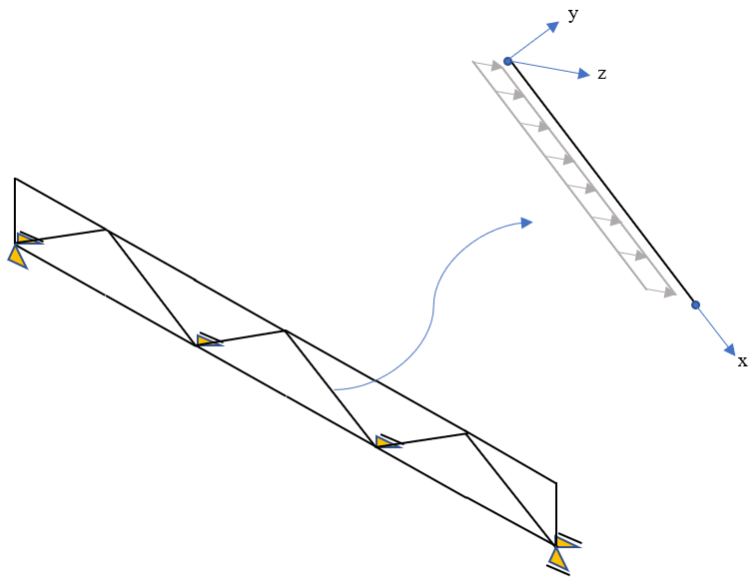

Figure 4.4: The wind load on a truss member

The type of deck considered in this thesis is a sandwich steel element, which means that the crowd load applied on the deck and the self-weight of the deck is transformed to the lower chord of the truss as a uniformly distributed load (see Figure 4.5).

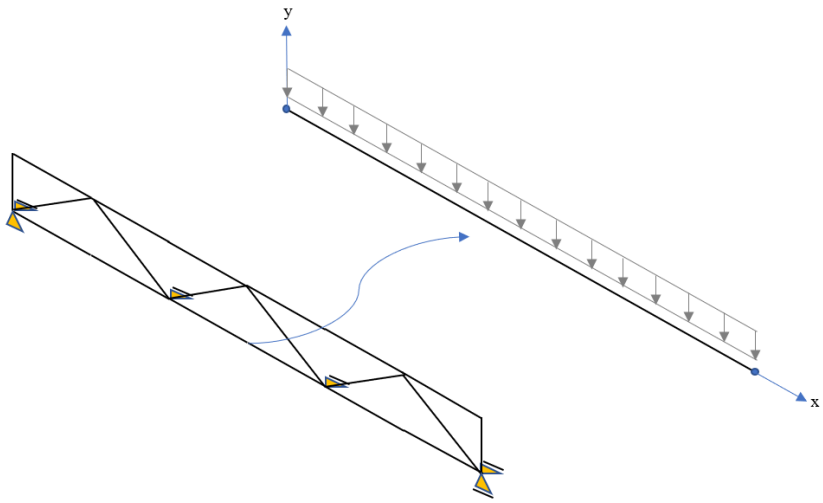

Figure 4.5: Loads from the bridge deck

4.1 Verification of Structural Model

To verify the simplification described in the previous section, a 3D bridge is modeled in Abaqus- a commercial finite element software (see Figure 4.6). The 3D model consists of two trusses with dimensions as shown in Figure 4.7 connected with cross-beams with a c-c distance of 1000mm. The bridge width is 3000mm. Quadratic elements, and fine mesh were used for the analysis. Three load cases are studied in this comparison:

- In the first analysis, the bridge under a uniformly distributed load is studied. The load is applied on the transverse beams as a line load with a magnitude of $q = 2.5N/mm$ for the first and the last beam, as they have half the tributary area, and $q = 5N/mm$ for the rest.
- In the second analysis a service vehicle is applied on the transverse beams using the model described in section 2.2.1, see Figure 4.8. The load is applied right next to one of the trusses resulting in the center of the outer forces being 100mm from the truss, to obtain the worst case.
- Finally, the wind load is applied on one truss as a line load with a magnitude of $q = 1N/mm$.

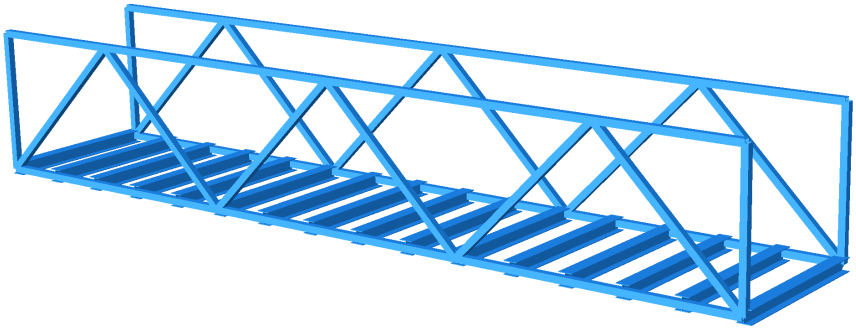

Figure 4.6: 3D truss in Abaqus

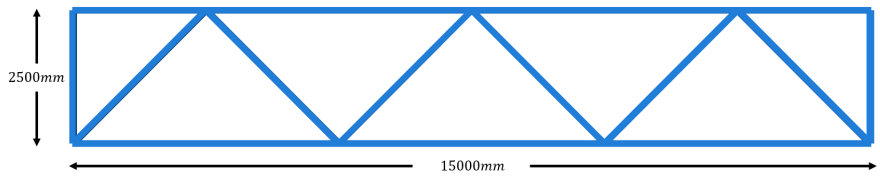

Figure 4.7: Truss dimensions in Abaqus

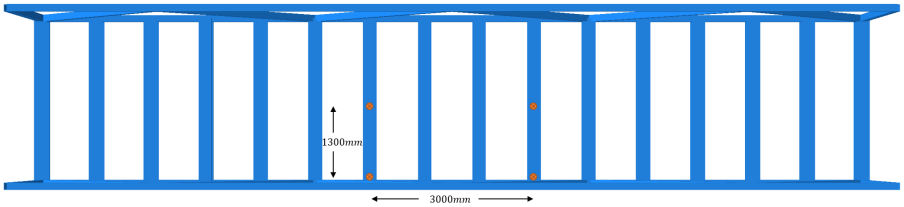

Figure 4.8: The Position of the Service Vehicle in the Abaqus Model

The boundary conditions for the 3D model are as shown in Figure 4.9. The figure shows a plan view of the bridge where in addition to the boundary conditions seen, all the corners are constrained in the y-direction.

Figure 4.9: Applied Boundary Conditions in Abaqus

A comparison is then done between the moments and the axial force diagrams of the upper and lower chord of the truss obtained from Abaqus and the developed script. Because the effects of the service vehicle are not to be accounted for in the SLS load combination, only the deformation induced by the uniformly distributed load and the wind load has been compared between Abaqus and the script.

In the first load-case, the diagrams in Figures 4.10 to 4.14 are in agreement with some differentiation in the moment diagram of the lower chord, see Figure 4.10. The difference in curve smoothness for the bending moment diagram in Figure 4.10 is due to the uniformly distributed load being applied on the transverse beams in Abaqus, acting like concentrated loads on the truss' lower chord, while it is acting directly as a line load on the lower chord of the truss in the script.

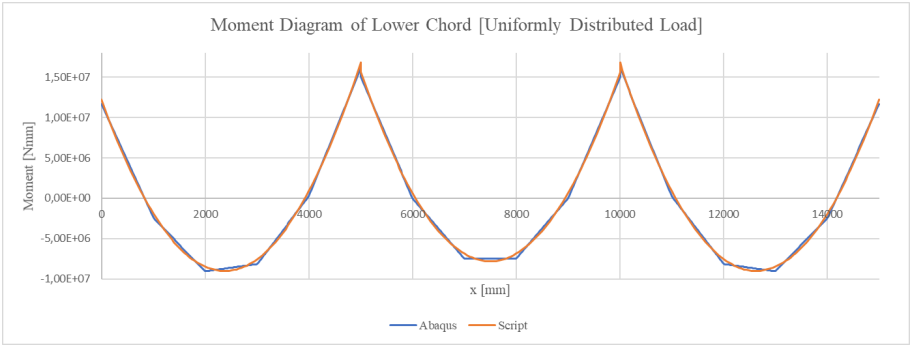

Figure 4.10: Moment Diagram of Lower Chord [Uniformly Distributed Load]

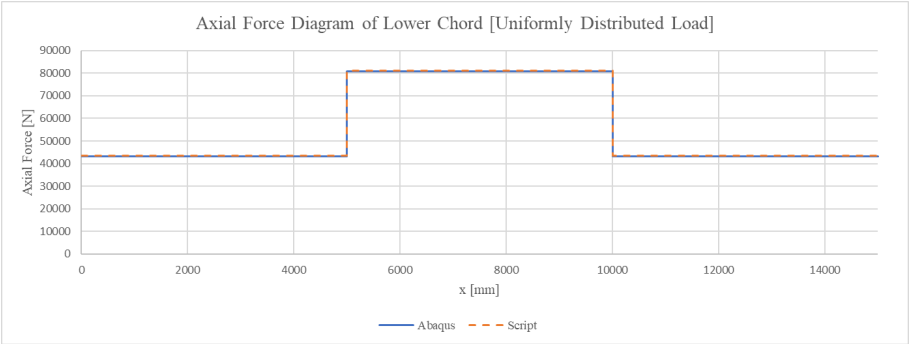

Figure 4.11: Axial Force Diagram of Lower Chord [Uniformly Distributed Load]

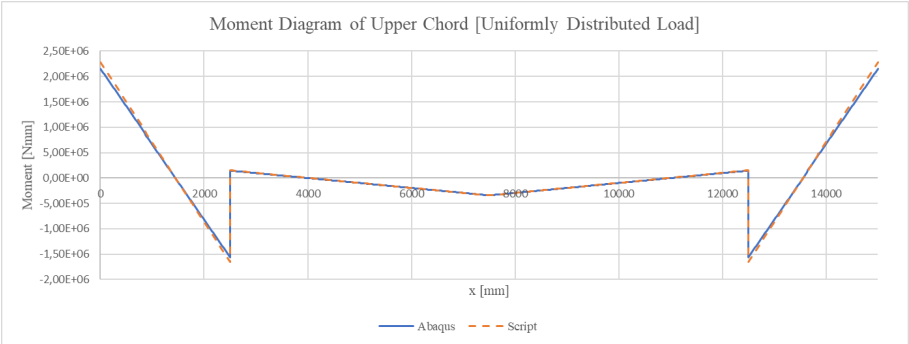

Figure 4.12: Moment Diagram of Upper Chord [Uniformly Distributed Load]

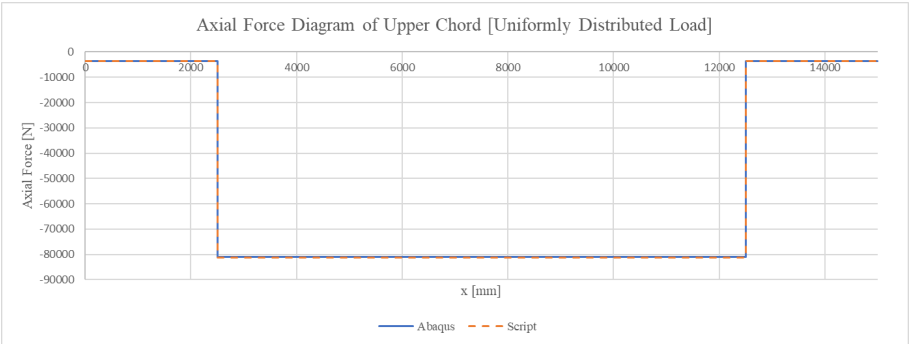

Figure 4.13: Axial Force Diagram of Upper Chord [Uniformly Distributed Load]

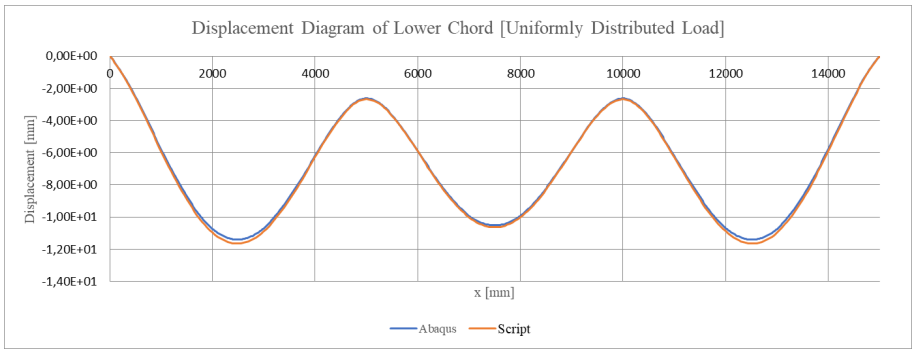

Figure 4.14: Displacement Diagram of Lower Chord [Uniformly Distributed Load]

Good agreement between the two models is also shown for the second load-case, as seen in Figures 4.15 to 4.18. However, for the axial diagram of the lower chord a difference as high as about 19% is observed in some locations. Because the rest of the results are in agreement and the script gives higher forces, these differences are acceptable.

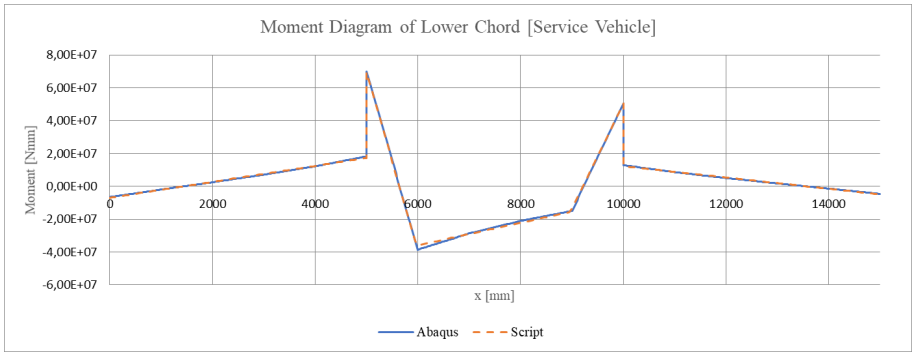

Figure 4.15: Moment Diagram of Lower Chord [Service Vehicle]

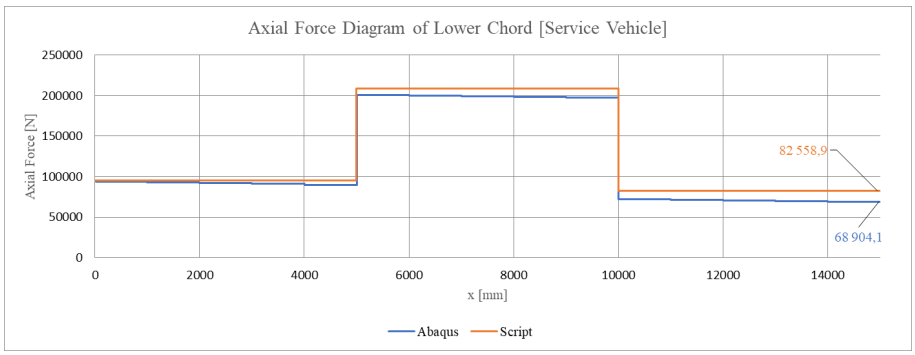

Figure 4.16: Axial Force Diagram of Lower Chord [Service Vehicle]

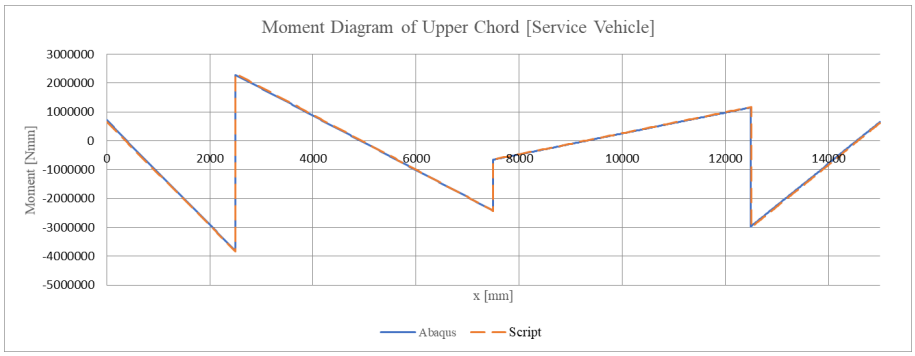

Figure 4.17: Moment Diagram of Upper Chord [Service Vehicle]

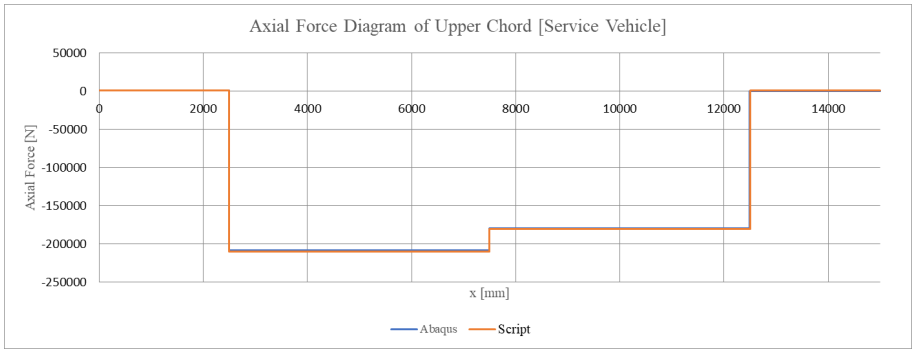

Figure 4.18: Axial Force Diagram of Upper Chord [Service Vehicle]

Regarding the last load-case, the 2D approximation starts to show bigger differences when the load is applied in the direction out-of-plane of the truss. For the moment diagram of a diagonal of a truss, in the script the moments obtained are higher near the connection to the lower chord (see Figure 4.19). The reason for this difference is that in the simplification done in the script, the lower chord is hindered from rotating around the x-axis (see Figure 4.2 Subfigure 4.21a) and thus the diagonals are acting like fixed beams in that connection. In reality, that connection would not be infinitely stiff but due to the large stiffness of the bridge deck, this assumption is justified. Another effect of that is seen in Figure 4.20, where the deflections are larger in the 3D-model.

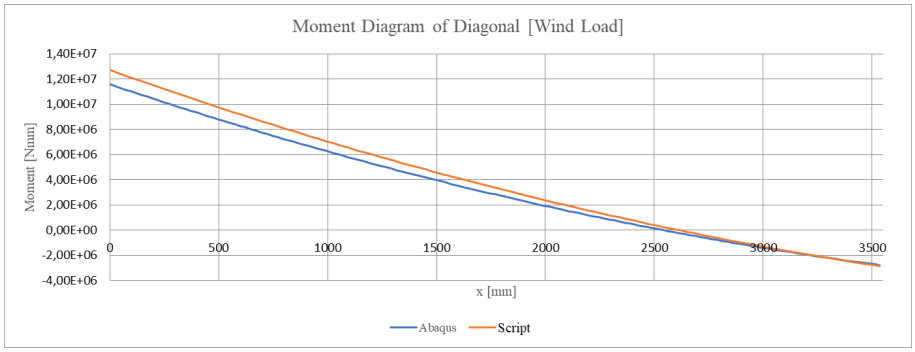

Figure 4.19: Moment Diagram of Diagonal [Wind Load]

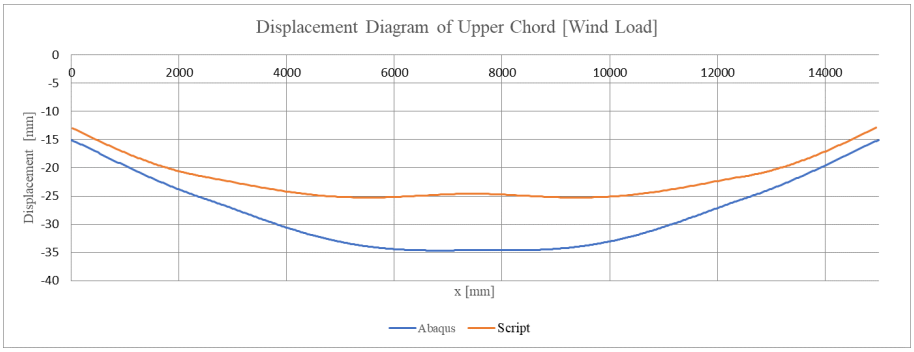

Figure 4.20: Out-of-Plane Displacement Diagram of Lower Chord [Wind Load]

Another effect of the 2D simplification is that in the script, the whole truss has a behavior of a fixed beam in the out-of-plane direction, see Subfigure 4.21a. Axial forces are induced in the upper chord of magnitude of 12kN, this applies to the lower chord also, and no axial forces are obtained from the script. A reason for this is that when a lateral load is acting on a fixed column as illustrated in Subfigure 4.21a, the column would deflect and no axial forces would be obtained. On the other side, the 3D bridge would act like a large beam that bends when affected by the wind load and this will result in compression on one truss and tension on the other one as seen in Subfigure 4.21b, and this is the reason why axial forces are induced in the 3D model. However, one other observation from the 3D model in Abaqus is illustrated in Subfigure 4.21c. Although the deck and the lower chords are acting like a beam in bending, where one lower chord is in compression and the lower chord on the other side of the deck is in tension, the upper chords are not following the same behavior and instead show the opposite, the upper chord closer to the load is in tension and the other one is in compression. The reason for that is that the center of rotation of the bridge is under the bridge as seen in Figure 4.21c and the external force will cause a rotation of the bridge, this will result in compression on the right truss and tension on the left truss which explains the behavior described before.

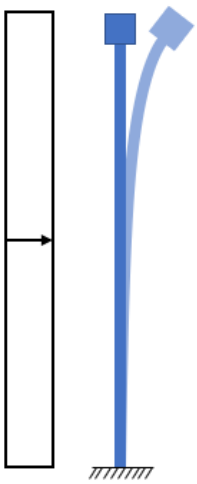

(a) Behavior of the 2D simplification of a truss

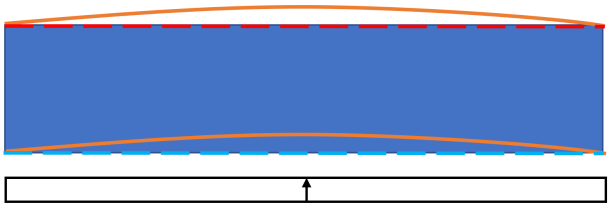

(b) Behavior of the 3D modeled bridge in Abaqus [Plan View]

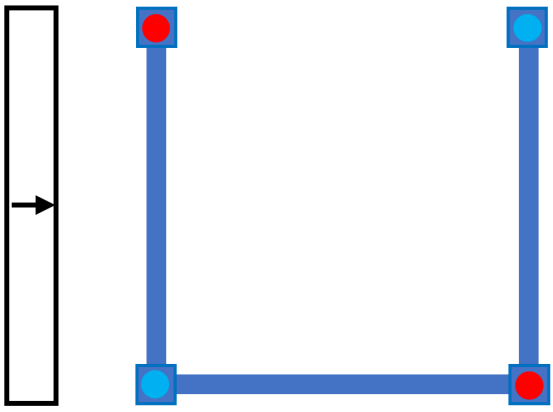

(c) Behavior of the 3D modeled bridge in Abaqus [Section View]

Figure 4.21: Comparison between the Behavior of a 2D and a 3D Model under Wind Load

Finally, the conclusion that can be drawn is that the approximation described in the previous section is accurate enough and can be used for analysis of truss bridges.

4.2 Python Program

The program to be used in this work is written in Python. The CALFEM finite element toolbox is used to create and solve FE-systems and calculate sectional forces in elements of the system. For optimization a genetic algorithm Python library is used.

4.2.1 Input

The input given to the program consists of material constants, geometry and loads. Material constants consists of Young's Modulus E, Shear Modulus G, Poisson's ratio v and the yield strength fy. All but yield strength, which depends on the steel grade to be used, are constant. The geometry is decided by the length L, the height H, the width B, number of divisions in the truss, distance between joints in the upper chord and the curvature of the upper chord. To decide which profile to be used in the members an index is given, representing a profile from a library of set profiles. Loads on members are given either as acting in the direction of the negative global y-axis or as distributed load acting in the direction of the members local x-,y-, or z-axes. The nodes can be loaded with point loads acting in the direction of the global x-,y-, and z-axes.

4.2.2 Parametric Model

A parametric model is built to generate different truss topologies. The parameters that govern the model are:

- L: the length of the truss.
- H_{min}: the minimum allowed height for the truss.
- H_{max}: the maximum allowed height for the truss.
- The number of divisions.
- The lengths of the divisions.

To generate a truss, the parametric model divides the upper and the lower chords into points, and then the verticals and the diagonals are connected between these points. For the case where the upper chord is curved, the sagitta (the distance between the center of an arc to the center of its base) is calculated by $s = H_{max} - (H_{min}$. Based on the sagitta, the radius of the circle is calculated using Equation 4.1 and then the coordinates of the upper chord's nodes are obtained using the circle equation in Equation 4.2 (See Figure 4.22).

$$r = \frac{s^2 + l^2}{2s} \tag{4.1}$$

$$(x - x_0)^2 + (y - y_0)^2 = r^2 \tag{4.2}$$

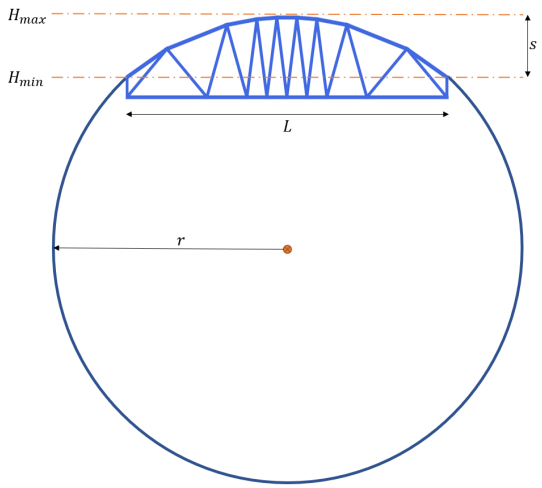

Figure 4.22: Method for deciding curvature of upper chord

By manipulating these parameters a large number of alternative topologies can be obtained. Some of these topologies are illustrated in Figure 4.23

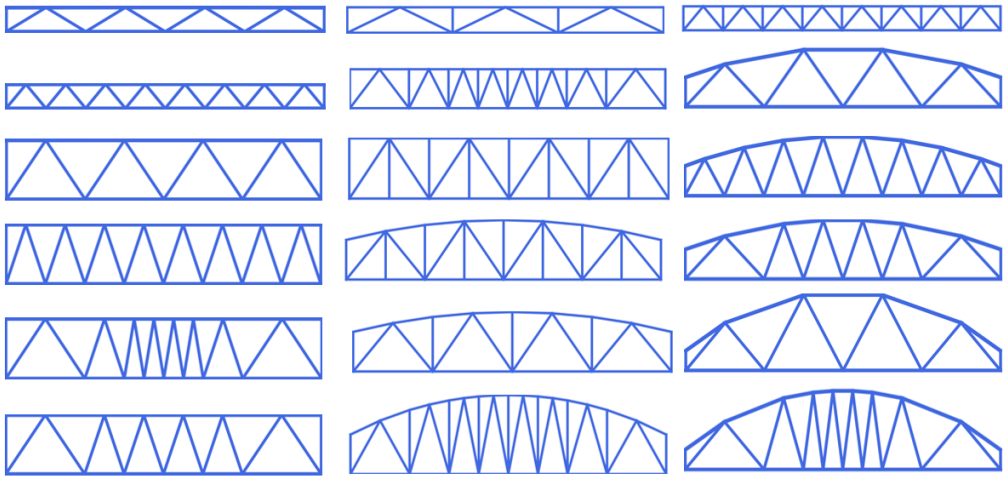

Figure 4.23: Example of Topologies that can be obtained from the Parametric Script

The way to decide the distance between joints in the lower chord with an even number of divisions are described in Equation 4.3-4.5 and Figure 4.24. For an odd number of divisons equation 4.4 is rounded up so that for the truss shown in Figure 4.25 n would be equal to 4.

$$a = [a_1, a_2, ...a_n] \tag{4.3}$$

$$n = \frac{\text{Number of divisons}}{2} \tag{4.4}$$

$$x_i = \frac{a_i * L/2}{\Sigma a} \tag{4.5}$$

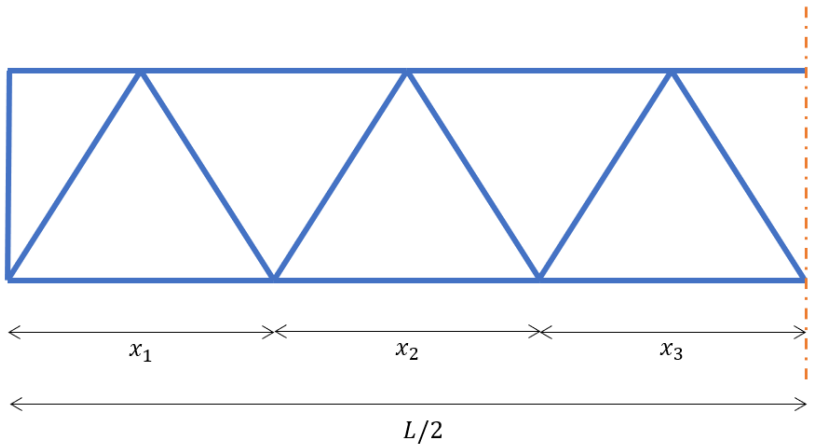

Figure 4.24: Division Length Distribution [Even Number of Divisions]

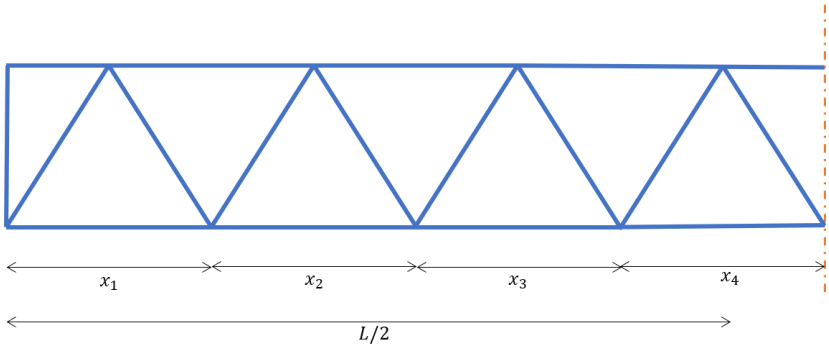

Figure 4.25: Division Length Distribution [Odd Number of Divisions]

Before continuing with a model for analysis in the optimization, the program checks if any angle in the truss is smaller than 30°, if that is the case no analysis is done on that truss and instead a large penalty is applied.

4.2.3 Finite Element Model

When the input is given the next step in the program is to group the members to know which members belong to the upper chord, the lower chord, diagonals and end posts. This is to be able to apply different loads and profiles to different parts of the truss. Now the members can be given start and end coordinates and cross-sectional properties based on the coordinates of the start and end nodes of the element and the index representing a profile in the library of set profiles. Each member is divided into eight elements in the finite element model to give accurate sectional forces and nodal displacements. The loads are applied to the elements and a stiffness matrix and force vector is created for the model. Together with the boundary conditions, the model can be solved and return nodal displacements and reaction forces.

4.2.4 Sectional Forces and Member Capacities

By extracting the element displacements from the nodal displacements, sectional forces in each element are calculated. In the start and end point of each element values are given representing six sectional forces;

- Normal force
- Shear along the y-axis
- Shear along the z-axis
- Torsion
- Moment around the y-axis
- Moment around the z-axis

Eight elements in each member means that there will be 16 values of each sectional force for each member. The maximum value out of these 16 will then be used for checking the utilization ratio in the members. To verify the utilization ratio the capacities in the members are calculated. Shear utilization and utilization in interaction between axial force and bending is returned for each member. Due to the facts that only hollow core sections are used and that they have such high torsional resistance, the members are assumed to have sufficient capacity to resist any torsion in the elements.

4.2.5 Global Analysis

After verifying the sectional forces against member capacities, a global analysis is conducted. First the maximum deflection in the direction of the global y-axis is extracted. Comparing this to the limit of allowed deflection L/400, returns a utilization ratio for deflection. The next step in the global analysis is to analyze the global buckling of the upper chord. Since the whole upper chord is in compression it can buckle out of plane both locally between joints but also globally, with a larger buckling length than the distance between the joints, with the joints acting as springs.

4.2.6 Optimization

For optimization the program will be used together with a python library for genetic algorithms. The program will be ran with four different load cases for each individual in the optimization. Firstly three different cases from ULS 6.10b (Table 2.8):

- Load Group 1 as Main Load
- Load Group 2 as Main Load with Service Vehicle in the middle of the span
- Load Group 2 as Main Load with the heavier axis of the Service Vehicle on the first Connection in the lower chord

In both cases the service vehicle is placed as close to the considered truss as possible. The fourth load combination is SLS 6.10ab (Table 2.9). The load case with the service vehicle on the first connection is assumed to be worse for the diagonals compared to when the service vehicle is in the middle of the span. Wind load as main load was assumed not to be the governing case and is not ran in the optimization to save time. To make sure that the assumption is valid the optimized bridge will

be tested with wind load as main load outside of the algorithm. For each load case the largest utilization ratio is stored and if any of the load cases give a value larger than one the individual will be given a penalty. Adding the weight of the individual with its eventual penalty gives the fitness of the individual.

The parameters in the optimization can take values between these intervals, where the max height parameter is set to 0% when a straight upper chord is used:

Parameter/Span	**20m**	**30m**	**40m**
Height	1400-2200	1400-2400	1400-2600
Maximum Height	0-5%	0-5%	0-5%
No. of Divisions	4-10	6-12	6-14

Where the maximum height is obtained by multiplying the percentage with the span of the bridge and then adding it to the height. The cross-sections used are presented in Appendix A

5
Results

The results from this work can be divided in two parts. One part where the program was ran to find suitable genetic algorithm parameters for this kind of optimization problem and another part where different types of trusses were compared.

5.1 Genetic Algorithm Parameters

In this part the truss for a bridge with a span of 20 meters and a width of three meters was studied with different values of genetic algorithm parameters. The parameters were:

- Number of generations
- Population size
- Mutation probability

Larger values of number of generations and population size would generally give better results but at the expense of computational time. This was expected since most algorithms will give better results if they are ran more thoroughly. However, it was noted that because of the randomness of the stochastic algorithm larger values of number of generations and population size did not always give a better result than smaller values, when comparing two runs of the algorithm. With this in mind it was decided, rather than running the algorithm once with large values of number of generations and population size, to run the algorithm several times with smaller values. Changing the mutation probability from the default value did not seem to affect the results for the better, probably because increasing it can lead to the algorithm not converging properly and decreasing it can lead to the algorithm getting stuck in local optima. The genetic algorithm parameters that were used for the studies in this work is shown in Table 5.1.

Table 5.1: Genetic Algorithm Parameters

Generations	100
Population Size	200
Mutation Probability	0.1

The value 0.1 for mutation probability means that there is a 10% chance for each gene in each individual to be replaced by a random value. Convergence criteria for the algorithm was that if the individual with the highest fitness in each generation

was not improved in 30 generations the algorithm stopped and gave the current result. It was assumed that if the convergence criteria was met, either the solution was stuck in a local optimum or the global optimum was reached. The initial idea was to run each optimization ten times with the same parameters to give reliable results despite the randomness of the algorithm, but after running the study of the effect of bent upper chord for 20 meters span(in a first study which is not presented, where the script was faulty), it was decided to change to five times with the same parameters. This was because some of the results from running it ten times were very similar to each other and hence fewer runs would give pretty much the same results but save a lot of time. By saving time more studies were able to be performed within the time scope of this work.

5.2 Effect of Bent Upper Chord

One of the truss topologies studied in this thesis is a truss with a bent upper chord as seen in Figure 5.1. To investigate if these toplogies would affect the optimization results in term of weight of the truss, a comparison study was conducted. In this study, a number of optimizations were ran using 3 different spans; a shorter span of 20 meters, an intermediate span of 30 meters and a longer span of 40 meters.

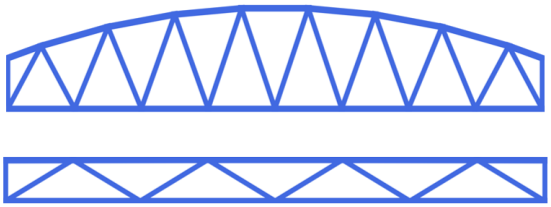

Figure 5.1: Truss Topologies with and Without Bent Upper Chord

As seen in Figure 5.2, where the weights are plotted next to each other in the order they were obtained, the weight tended to decrease when a bent upper chord was allowed in the optimization. For every case but one, the truss with bent upper chord was lighter. However, this is because of the randomness in the genetic algorithm and the results are better interpreted by looking at the tendency and the comparison between the lightest trusses in both cases. In Table 5.2 the lightest trusses are compared and the truss with bent upper chord was found to be 5.2% percent lighter than the truss without bent upper chord.

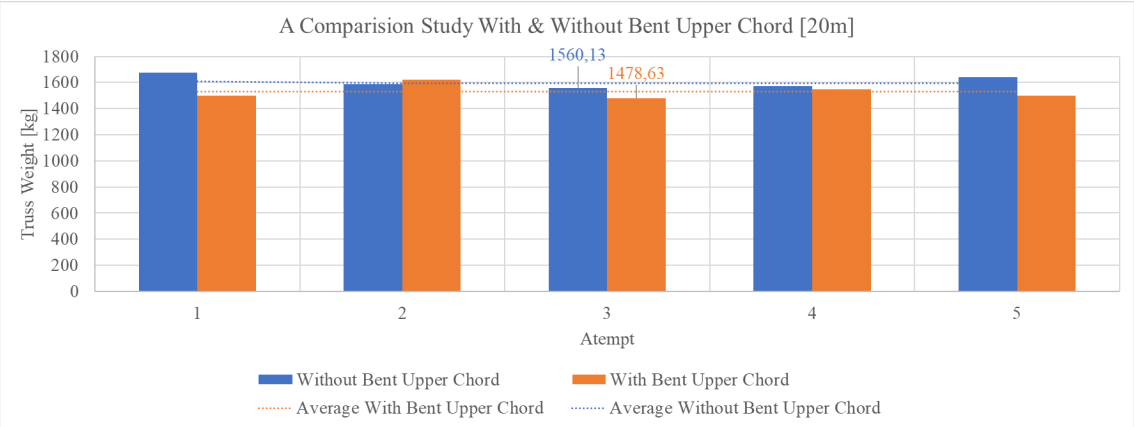

Figure 5.2: A Comparision Study with & without Bent Upper Chord [20m Span]

For an intermediate span of 30 meters the weights are plotted in Figure 5.3 in the same way as for the 20 meters span. For this span length the weight difference was 8.9% as seen in Table 5.2 which indicates a larger potential for weight savings for an intermediate span.

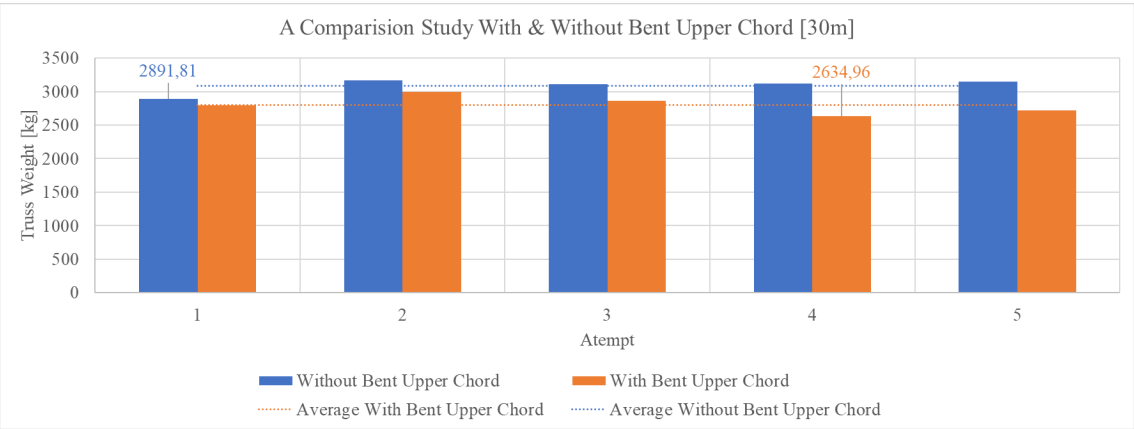

Figure 5.3: A Comparision Study with & without Bent Upper Chord [30m Span]

For the longer span of 40 meters, the difference between the lightest trusses obtained with and without upper chord was 9.3%, see Table 5.2. As can be seen in the plotted weights in Figure 5.4 the trusses with bent upper chord tends to be lighter than the ones without in all the ran optimizations, which was the case for 30 meters as well.

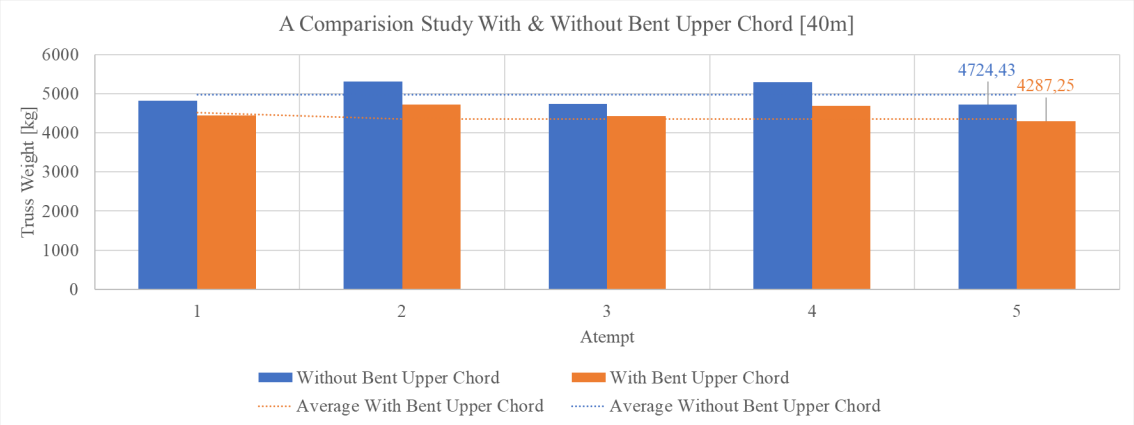

Figure 5.4: A Comparision Study with & without Bent Upper Chord [40m Span]

In Table 5.2 a summary of the weight difference for the study with and without bent upper chord can be seen.

Table 5.2: Weights of optimized trusses

Span [m]	**20**	**30**	**40**
Weight without Bent Upper Chord [kg]	1560.13	2891.81	4724.43
Weight with Bent Upper Chord [kg]	1478.63	2634.96	4287.25
Difference [%]	5.2	8.9	9.3
Difference [kg]	81.5	256.85	437.18

The parameters chosen by the genetic algorithm and the utilization ratios for the lightest trusses are presented in Table 5.3 and Table 5.4. In Figures 5.5 to 5.7, plots of the lightest trusses are shown where the members with the highest utilization ratio are highlighted.

Table 5.3: Optimized Truss without Bent Upper Chord

Span [m]	**20**	**30**	**40**
Height [mm]	1650	2000	2050
Cross-section - Upper Chord	150*150*6.0	200*200*6.0	250*250*6.0
Cross-section - Diagonals	120*120*5.0	120*120*5.0	140*140*5.0
Cross-section - Lower Chord	150*150*5.0	160*160*6.0	200*120*8.0
Cross-section - End Verticals	80*40*5.0	100*60*5.0	70*70*5.0
Highest UR- Upper Chord [%]	77.9%	72.9%	79.6%
Highest UR- Diagonals [%]	53.9%	66.6%	77.0%
Highest UR- Lower Chord [%]	95.5%	98.1%	99.5%
Highest UR- End Verticals [%]	16.1%	13.3%	19.0%
UR - Global Buckling [%]	97.8%	96.0%	99.9%

From Table 5.3 it can be seen that overall global buckling was observed to be the most critical check with the highest utilization ratio. The lower chords were

also utilized with high values. The diagonals and upper chord had lower utilization ratios compared with the lower chord. The reason why smaller cross-sections can't be used for the upper chord and the diagonals is because of their importance for giving stiffer springs when checking the global buckling. Finally, the end verticals were the members with the lowest utilization ratio.

Table 5.4: Optimized Truss with Bent Upper Chord

Span [m]	**20**	**30**	**40**
Height [mm]	1450	1400	1750
Maximum Height [mm]	2000	2600	3400
Cross-section - Upper Chord	150*150*6.0	160*160*6.0	180*180*6.0
Cross-section - Diagonals	150*100*4.0	120*120*5.0	140*140*5.0
Cross-section - Lower Chord	140*140*5.0	180*100*6.0	150*150*6.0
Cross-section - End Verticals	80*40*5.0	50*50*5.0	90*50*5.0
Highest UR- Upper Chord [%]	63.3%	73.7%	62.3%
Highest UR- Diagonals [%]	65.4%	50.8%	52.6%
Highest UR- Lower Chord [%]	94.3%	92.6%	96.5%
Highest UR- End Verticals [%]	17.1%	16.6%	13.4%
UR - Global Buckling [%]	94.9%	98.1%	95.6%

The same applies for the truss obtained with bent upper chord as seen in Table 5.4. However, the utilization ratios of the diagonals are lower compared to the utilization ratios obtained from the truss without bent upper chord. For the longest span without upper chord the utilization ratio for the diagonals was 77% where for the same span with bent upper chord it was approximately 53% .This decreased utilization ratio for the diagonals is combined with smaller cross-sections for the upper chord, and even the lower chord had a smaller cross-section. This due to the deeper truss in the middle which gives a larger lever arm to take care of the moments and thus lower axial forces in the lower and upper chord. This indicates that for longer spans, higher trusses are beneficial.

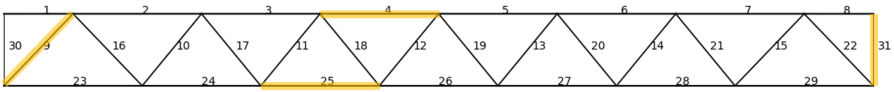

(a) Optimized Truss without Bent Upper Chord

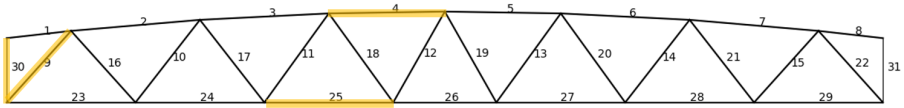

(b) Optimized Truss with Bent Upper Chord

Figure 5.5: Optimized Truss for 20m span

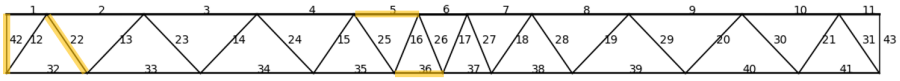

(a) Optimized Truss without Bent Upper Chord

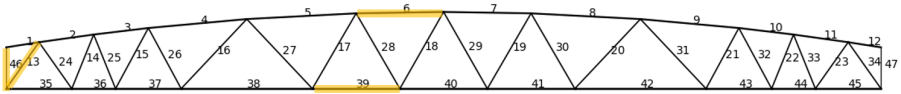

(b) Optimized Truss with Bent Upper Chord

Figure 5.6: Optimized Truss for 30m span

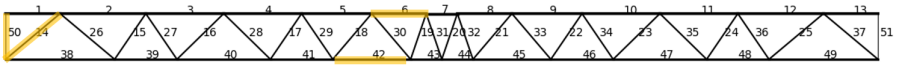

(a) Optimized Truss without Bent Upper Chord

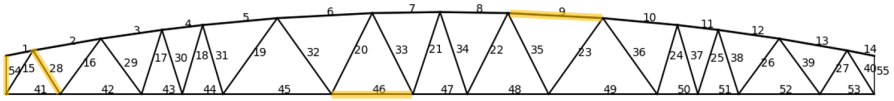

(b) Optimized Truss with Bent Upper Chord

Figure 5.7: Optimized Truss for 40m span

In Figure 5.8 to Figure 5.10, the member weights distribution is plotted for the best trusses obtained with and without bent upper chord. For the 20 meter span we see that the upper chord and the diagonals stand for approximately 70% of the weight of the truss, yet these members are not fully utilized. The same applies for the intermediate and the longer span. As seen in Figure 5.9 the upper chord and the diagonals stand for about 70% of the weight. However, with increased span length when we have bent upper chord, the diagonals starts to get a higher portion of this 70%, for instance for the 40 meters span, the diagonals stands for 44% of the weight, where their contribution was 34% for the shorter span and 38% for the intermediate span. This is because the diagonals are longer for trusses with bent upper chord due to higher height in the middle of the truss.

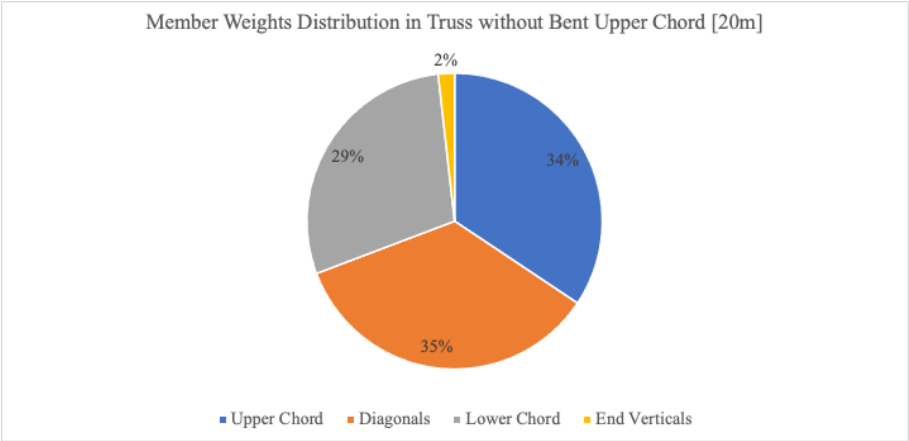

(a) Member Weights Distribution in Truss without Bent Upper Chord [20m]

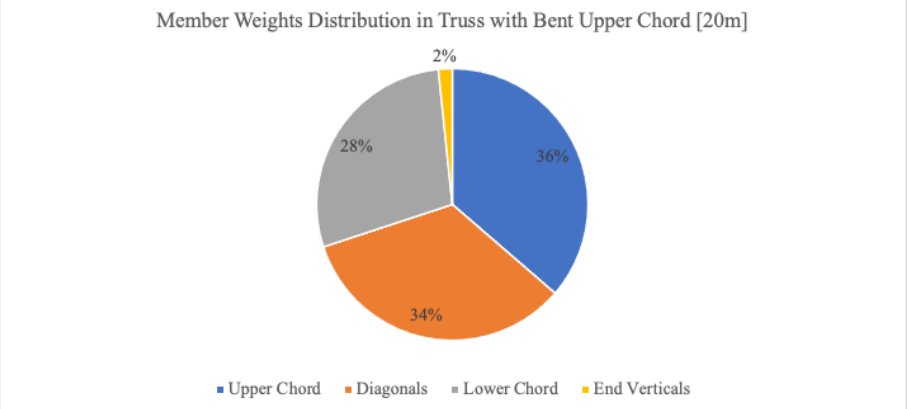

(b) Member Weights Distribution in Truss with Bent Upper Chord [20m]

Figure 5.8: Member Weights Distribution for 20m span

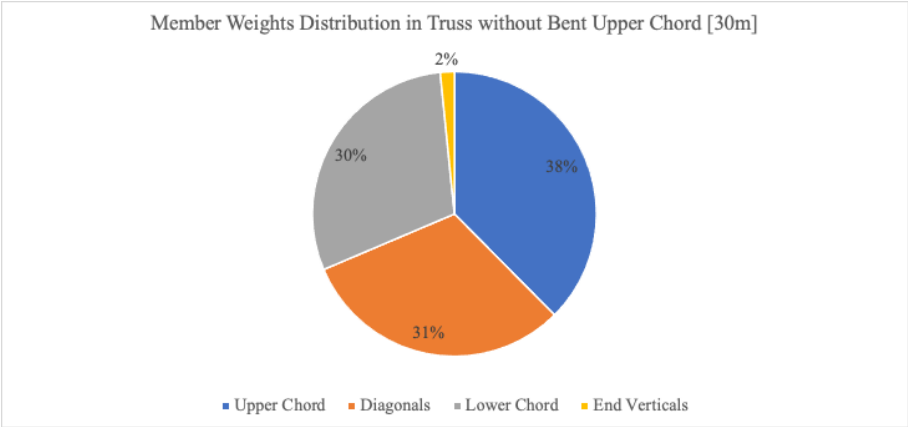

(a) Member Weights Distribution in Truss without Bent Upper Chord [30m]

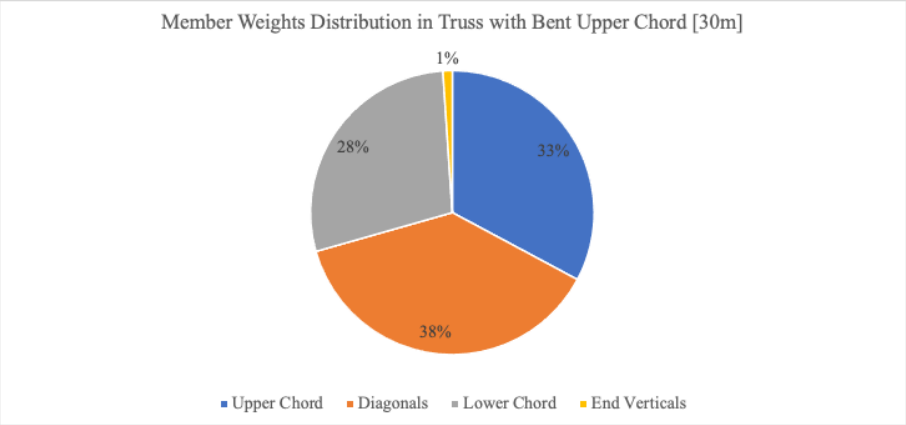

(b) Member Weights Distribution in Truss with Bent Upper Chord [30m]

Figure 5.9: Member Weights Distribution for 30m span

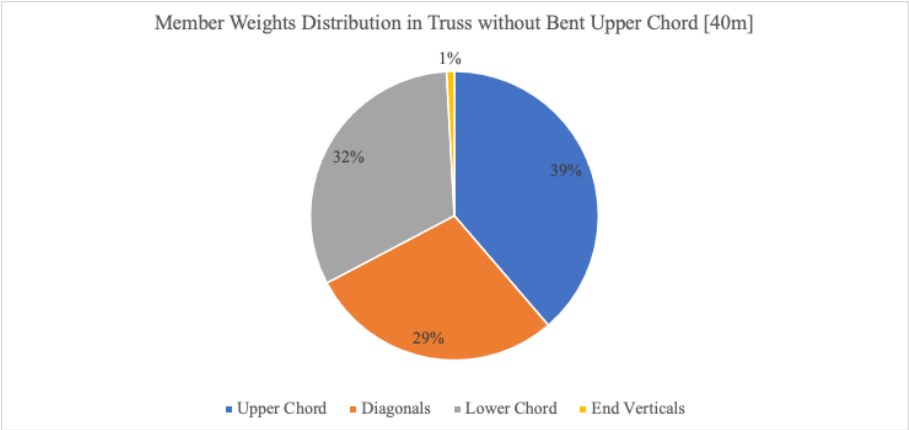

(a) Member Weights Distribution in Truss without Bent Upper Chord [40m]

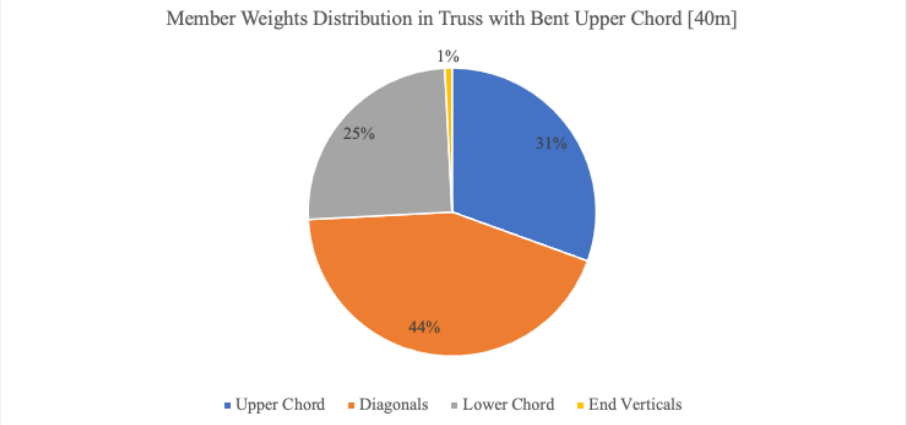

(b) Member Weights Distribution in Truss with Bent Upper Chord [40m]

Figure 5.10: Member Weights Distribution for 40m span

5.3 Effect of Higher Steel Grade

The effect of using steel with higher grade was studied. In this case only trusses without bent upper chords were studied with 3 different spans, a shorter span of 20 meters, an intermediate span of 30 meters and a longer span of 40 meters. The steel grade used is s500 where the yield strength of the steel is $f_y = 500MPa$. Furthermore, for this grade of steel large suppliers only store cold formed sections and thus only KKR profiles are studied. This was done by using the same profile data base and using the buckling curves related to cold formed sections.

For the case with the shorter span(Figure 5.14, a difference of 12.3% is obtained with the higher steel grade as seen in table 5.5.

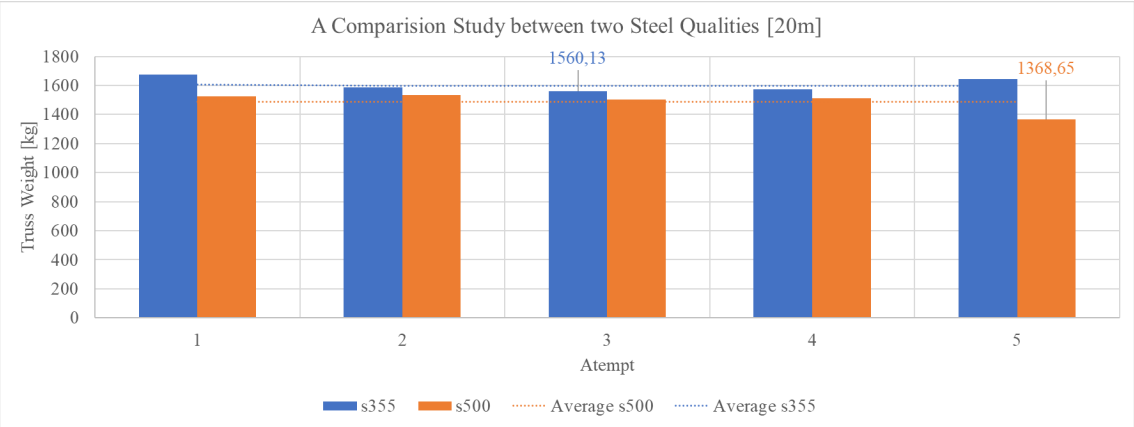

Figure 5.11: A Comparison Study with s355 and s500 Steel Grades [20m Span]

The intermediate span benefited a bit less, 4.0%, as seen in Table 5.5 and Figure 5.15

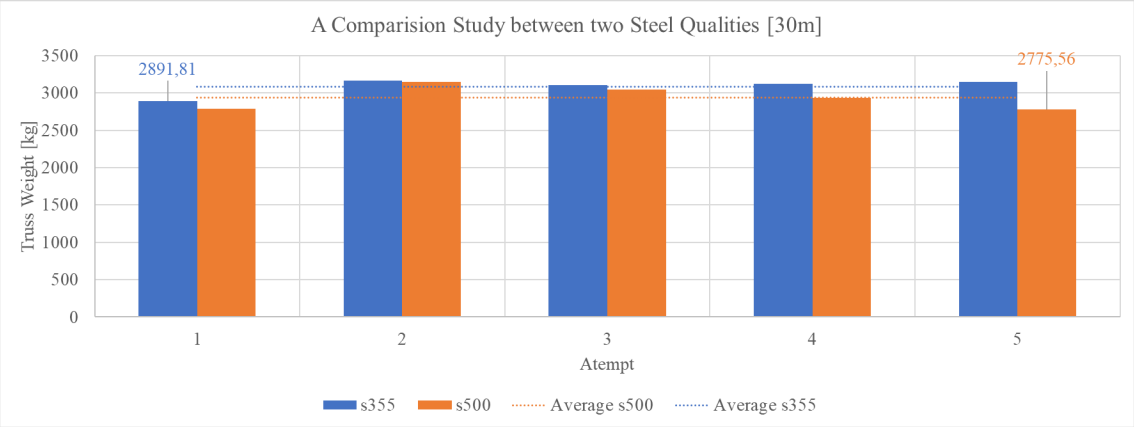

Figure 5.12: A Comparison Study with s355 and s500 Steel Grades [30m Span]

For the long span the weight decrease was only 1.2% and as can be seen in Figure 5.16 the weight was lower for the lower steel grade in some cases when comparing the optimizations in the order they were ran.

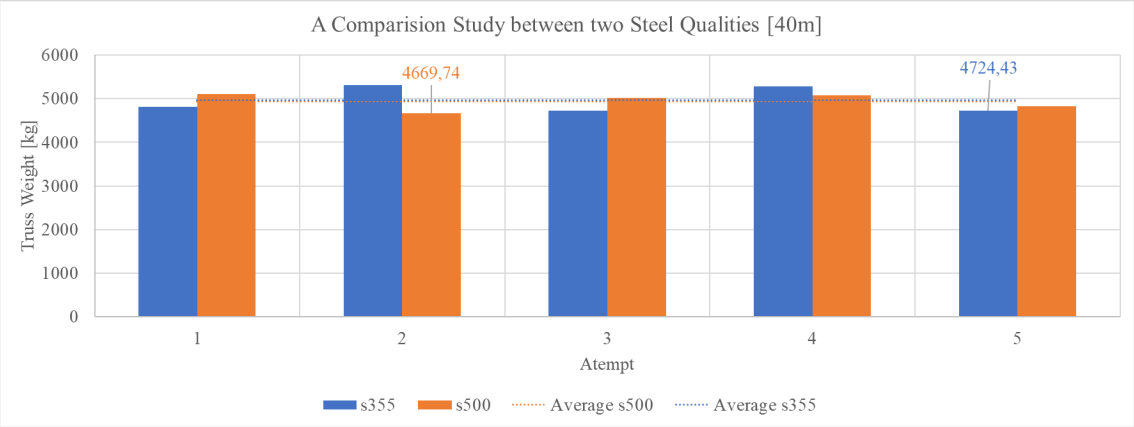

Figure 5.13: A Comparison Study with s355 and s500 Steel Grades [40m Span]

In Table 5.5 a summary of the weight difference for the study with hot-rolled s355 and cold-formed s500 can be seen.

Table 5.5: Weights of optimized trusses

Span [m]	**20**	**30**	**40**
Weight with s355 [kg]	1560.13	2891.81	4724.43
Weight with s500 [kg]	1368.65	2775.56	4669.74
Difference [%]	12.3	4.0	1.2
Difference [kg]	191.48	116.25	54.69

In Table 5.6 the parameters and utilization ratios of the optimized s500 trusses can be seen. The utilization in the lower chord becomes lower for the intermediate and the longer span.

Table 5.6: Optimized Truss with s500 Steel

Span [m]	**20**	**30**	**40**
Height [mm]	1850	1750	2050
Cross-section - Upper Chord	160*160*6.0	220*220*6.0	250*250*6.0
Cross-section - Diagonals	100*100*4.0	120*120*5.0	150*150*5.0
Cross-section - Lower Chord	160*80*4.0	200*100*5.0	180*180*6.0
Cross-section - End Verticals	80*80*5.0	50*50*5.0	50*50*5.0
Highest UR- Upper Chord [%]	52.9%	59.7%	67.3%
Highest UR- Diagonals [%]	73.8%	51.6%	39.1%
Highest UR- Lower Chord [%]	98.8%	79.2%	82.7%
Highest UR- End Verticals [%]	12.6%	10.8%	10.0%
UR - Global Buckling [%]	99.5%	100.0%	92.7%

In Figure 5.14 to 5.16 the optimized trusses for both steel grades for each span are shown. It can be noted that for s500 the number of divisions in the truss is higher for all of the spans.

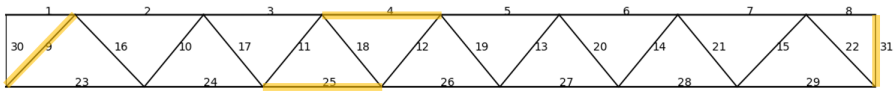

(a) Optimized Truss with s355

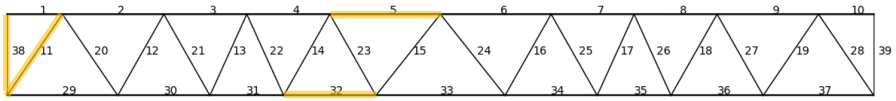

(b) Optimized Truss with s500

Figure 5.14: Optimized Truss for 20m span

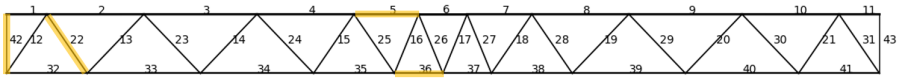

(a) Optimized Truss with s355

(b) Optimized Truss with s500

Figure 5.15: Optimized Truss for 30m span

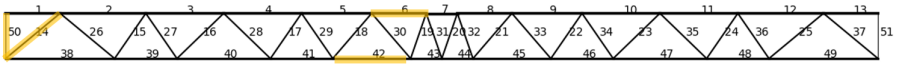

(a) Optimized Truss with s355

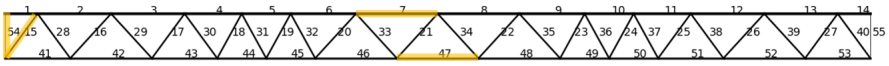

(b) Optimized Truss with s500

Figure 5.16: Optimized Truss for 40m span

Looking at Figure 5.17 to 5.19 the weight distribution for s355 and s500 are compared. For the shorter span a larger portion of the weight is in the upper chord for s500 compared to s355. In the intermediate and longer span the weight distribution is similar for s355 and s500.

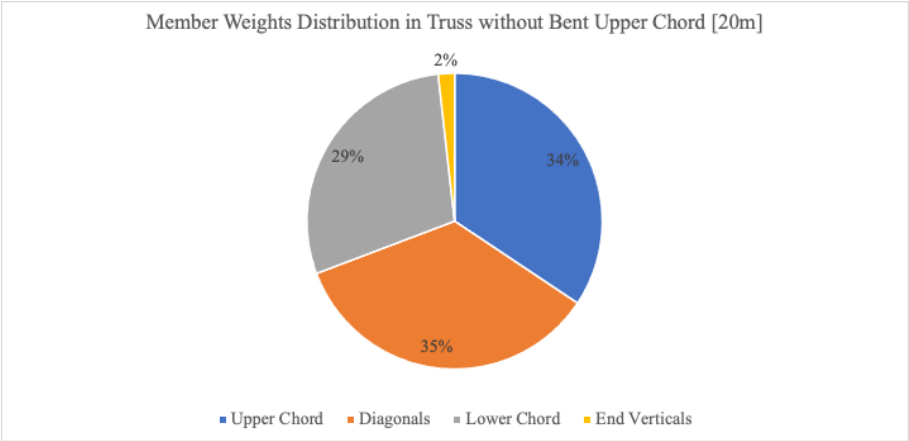

(a) Member Weights Distribution in Truss with s355 [20m]

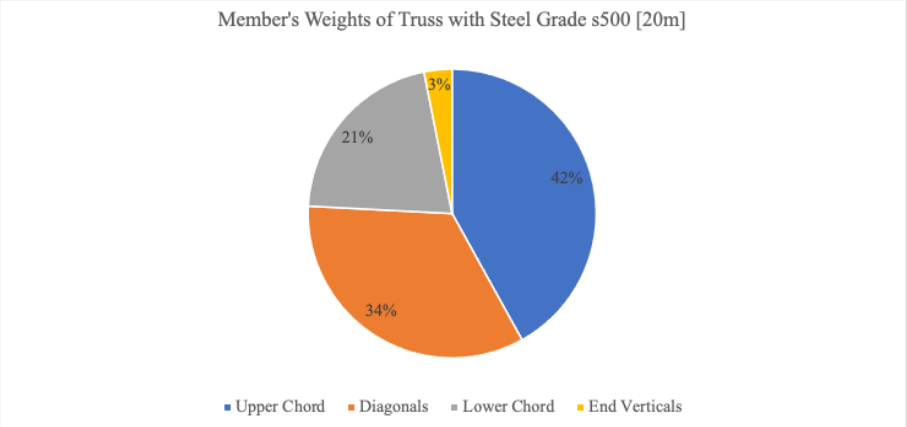

(b) Member Weights Distribution in Truss with s500 [20m]

Figure 5.17: Member Weights Distribution for 20m span

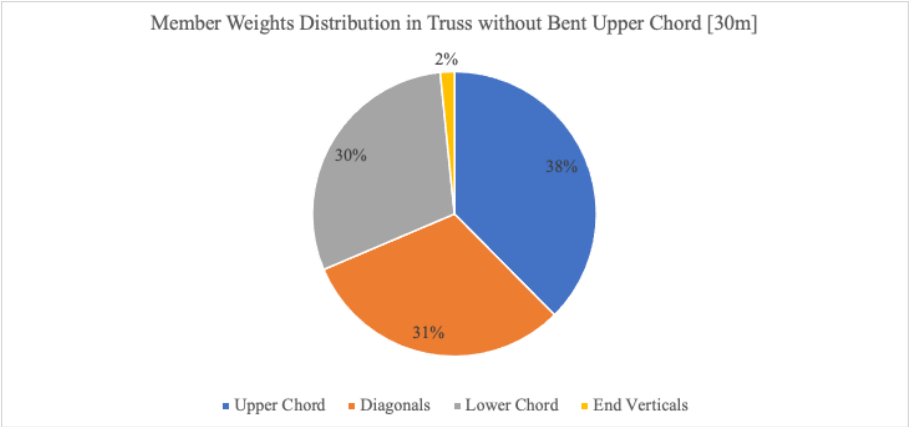

(a) Member Weights Distribution in Truss with s355 [30m]

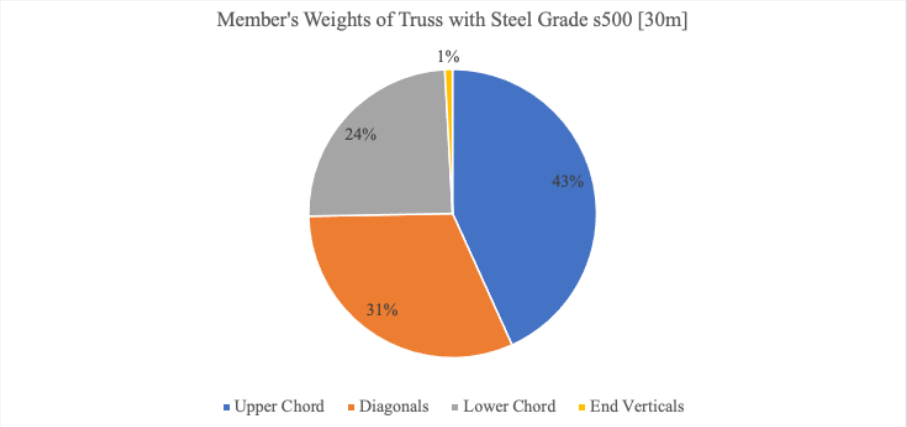

(b) Member Weights Distribution in Truss with s500 [30m]

Figure 5.18: Member Weights Distribution for 30m span

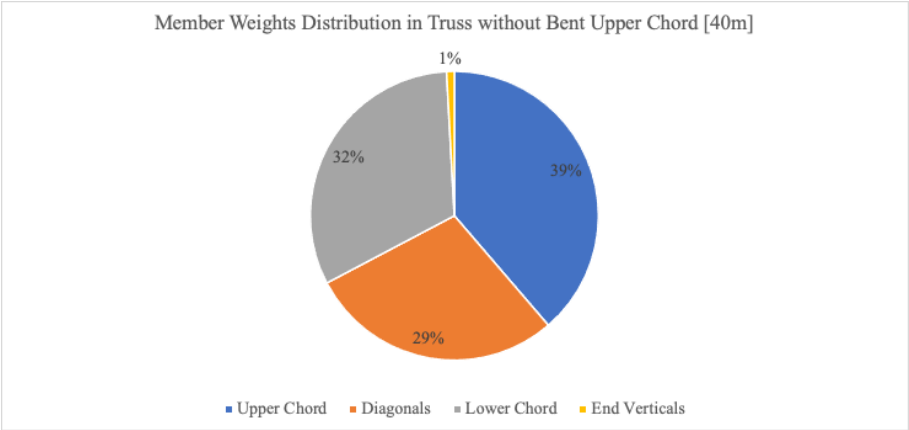

(a) Member Weights Distribution in Truss with s355 [40m]

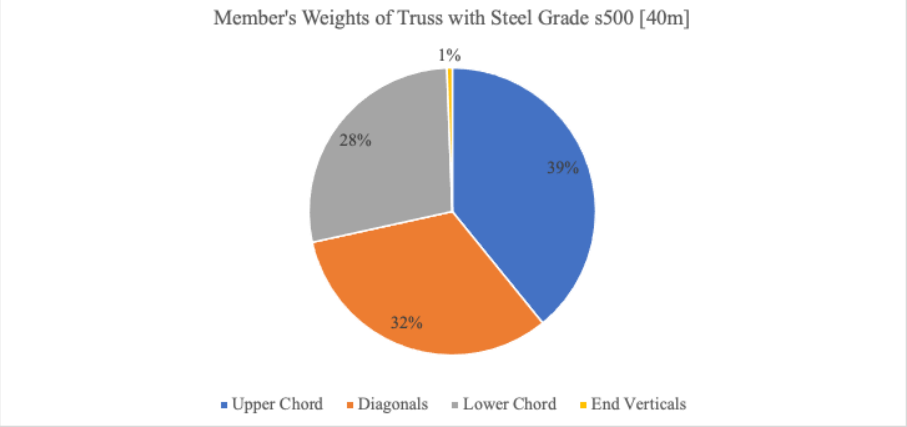

(b) Member Weights Distribution in Truss with s500 [40m]

Figure 5.19: Member Weights Distribution for 40m span

6
Discussion

6.1 Effect of Bent Upper Chord

As seen in the previous sections, in all the cases the trusses with bent upper chord showed lower weights, the longer the span the higher the difference. For the shortest span the difference was 5.2%, where for intermediate span 8.9%, and for the longest span 9.3%. The number of divisions didn't change for the first case with the shortest span, for the intermediate and the longer span the genetic algorithm have chosen one extra division for the bent upper chord cases. Furthermore, looking at the heights obtained, for the cases with the bent upper chord the heights in the edges are always lower than the constant height in the trusses without bent upper chord. This shows how the genetic algorithm utilize a higher height in the middle of the truss where the bending moments are high and thus a deeper truss is needed.

Overall, the global buckling was observed to be the most critical check with the highest utilization ratio. The upper and the lower chords were also utilized with high values. The diagonals had lower utilization ratios compared with the upper and the lower chord. The reason why smaller cross-sections can't be used is because of the diagonals importance for giving stiffer springs when checking the global buckling. Finally, the end verticals were the members with the lowest utilization ratio.

Span [m]	**20**	**30**	**40**
Height without Bent Upper Chord [mm]	1650	2000	2050
End Height with Bent Upper Chord [mm]	1450	1400	1750
Max Height with Bent Upper Chord [mm]	2000	2600	3400
No of Divisions without Bent Upper Chord	7	10	12
No of Divisions with Bent Upper Chord	7	11	13
Difference in Weight [%]	5.2	8.9	9.3

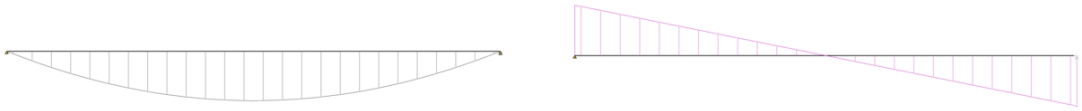

(a) Moment and Shear Diagram of a beam with a Uniformly Distributed Load

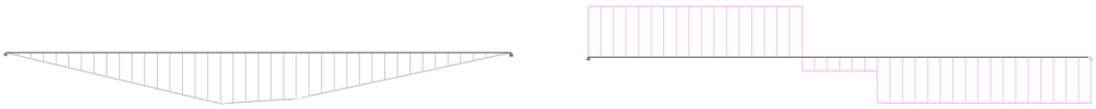

(b) Moment and Shear Diagram of a beam with a Service Vehicle positioned in the middle

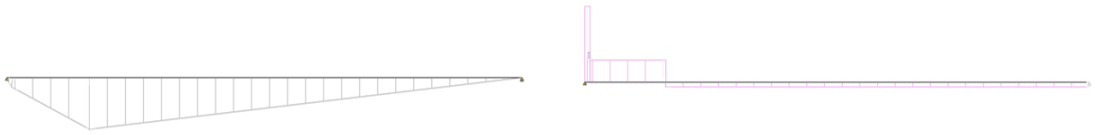

(c) Moment and Shear Diagram of a beam with a Service Vehicle positioned near the edge

Figure 6.1: Forces in a beam under three Load Cases

Furthermore, differences in the weight and highest utilization ratios are noticed between the result obtained from the genetic algorithm, where the distances between the divisions in the truss are not equal, and the same truss where the distances are afterward changed to be equal. One reason for this is that the formula for calculating the spring stiffness in the global buckling checks used in the Eurocode is using the average stiffness and even the the average difference between the springs is used. This indicate that a more precise way to calculate the global buckling may show a more pronounced effect of the distance between the divisions and thus give a favorable effect of using uneven distances between the divisions.

Span [m]	**20**	**30**	**40**
Weight with uneven distances [kg]	1478.63	2634.96	4287.25
Highest UR with uneven distances [%]	94.9	98.1	95.6
Weight with even distances [kg]	1477	2657.44	4306.41
Highest UR with even distances [%]	93	106	99

6.2 Effect of Higher Steel Grade

From the results it could be seen that for all spans the weight tended to decreased when s500 was used. For the higher steel grade the percentual weight difference decreased with longer spans and for 40 meters the results intended that there was almost no benefit at all when increasing the steel grade. For 20 meters however, the results intended that there is a lot to gain from a weight perspective when using a higher steel grade. For longer spans the global buckling length of the upper chord

increases and the benefits of having higher yield strength will be smaller compared to the negative effect of the higher buckling-curve factor. In the equation for the critical buckling load the length is squared making the trusses exponentially become more sensitive to the worse buckling resistance with increasing span length. Other than buckling the capacities of the bridge is increased without any drawbacks, which should lead to better potential for weight decrease in shorter spans, which is what the results intended.

The higher buckling factor for cold-formed profiles makes the trusses more sensitive to global buckling and the low utilization ratios in the diagonals and upper chord that can be seen in Table 5.6 indicates that they, as for the cases with and without bent upper chord too, mainly stiffen the upper chord against global buckling. What can be seen in Table 5.6 though is that the lower chord also gets lower utilization, indicating that even the lower chord needs to have a cross-section larger than is necessary to resists its internal forces, just to stiffen the upper chord against global buckling. From Table 5.6 it can be noted that the utilization ratio in the upper chord is lower for s500 than for s355, see Table 5.3. This indicates that the global buckling is even more critical for higher steel grades with cold-formed profiles and that the upper chord is more overdesigned, with regard to the buckling between joints in the upper chord, to counteract the global buckling.

The fact that the optimized truss for s500 had more divisions for all spans is another indication of global buckling being critical since more divisons means more joints stiffening the upper chord against global buckling. So rather than decreasing the number of members the weight is lowered thanks to the possibility of using smaller cross-section when having higher grade steel. This was expected due to higher buckling curve factor for cold-formed profiles, decreasing the resistance to buckling which was already the most critical action in the bridge. For the diagonals it was noted that the utilization ratio decreased with increased span lengths for s500. This is another indication that the global buckling is most critical and that the span of the truss amplifies its effect. The longer the span the less the diagonals are fitted to resist their internal forces and instead acting as stiffeners to the upper chord.

In Figure 5.17 the weight distribution is more in the upper chord for s500 for the 20 meter span. Since the steel is stronger the internal forces will be less critical and more weight will be needed in the upper chord to compensate for the worse buckling factor.

6.3 Structural Model

The 2D structural model used had some limitations regarding treatment of torsional effects. Other than this the used model gave similar results as the 3D model. Going into this work it was not certain wether the model should be in 2D or 3D but the verifications that were done show that it is possible to simplify to 2D. This can save computational time and also removes the need to model the bridge deck when analyzing a truss.

7
Conclusion

The aim of the thesis was to develop a parametric program that generates steel truss girders used in pedestrian bridges, analyze them and optimize them using genetic algorithm. In Addition, doing comparisons to evaluate how certain topologies and steel grades affect the results. The results indicated a number of things:

i A bent upper chord had a pronounced effect on the truss weight in intermediate and larger spans, and a noticeable effect on the shorter spans.
ii Genetic algorithms are a good tool to optimize these trusses, but one drawback when used in the programming language python is their long computational time.
iii Global buckling is the main factor restricting the use of smaller cross-sections for the diagonals and the upper chord.
iv Higher steel grade has a significant effect on the truss weight for shorter spans but for intermediate and longer spans the effect decreases.
v A 2D simplification is possible when optimizing trusses.

7.1 Further Studies

In this section some suggestions to improve the work are presented:

- The possibility to add more supports to investigate continuous truss over more than one span.
- Investigating the effects of temperature loads & the dynamic response on the optimization results.
- Adding the additional effects of the 3D-analysis to the 2D-model.
- Overlooking the program to increase the speed.
- Include the economical aspect in the optimization.
- Include the possibility for the outermost diagonals to start from the upper chord.
- Investigate the effect of modified warren on global buckling.

Bibliography

Ajouz, R. (2007). Parametric design of steel structures - fundamentals of parametric design using grasshopper. *Steel Construction*, *14*(3), 185–195. https://doi.org/10.1002/stco.202100011

Andreas, K. (2013). *Pedestrian bridges : Ramps, walkways, structures*. Detail Business Information GmbH.

Baldock, R. (2007). *Structural optimisation in building design practice: Case-studies in topology optimisation of bracing systems* (Doctoral dissertation). Cambridge University.

Boverket. (2021). *Miljöindikatorer – aktuell status*. https://www.boverket.se/sv/byggande/hallbart-byggande-och-forvaltning/miljoindikatorer---aktuell-status/ (accessed: 2022-04-23)

Brockenbrough, R. L., & Merritt, F. S. (2016). *Structural steel designer's handbook* (6th ed.). McGraw Hill Education.

Ching, E., & Carstensen, J. V. (2022). Truss topology optimization of timber–steel structures for reduced embodied carbon design. *Engineering Structures*, *252*.

Debney, P. (2020). *Computational engineering*. The institution of structural engineers.

DeCelle, J. et al. (2013). *WPI-Pedestrian Bridge Study*.

Gardner, L., Saari, N., & Wang, F. (2010). Comparative experimental study of hot-rolled and cold-formed rectangular hollow sections. *Thin-Walled Structures*, *48*(7), 495–507. https://doi.org/https://doi.org/10.1016/j.tws.2010.02.003

Hanses, K. (2015). *Basics steel construction*. Birkhäuser.

Hirt, M., & Lebet, J.-P. (2013). *Steel bridges: Conceptual and structural design of steel and steel-concrete composite bridges* (1st ed.). EPFL Press.

Holland, J. H. (1992). Genetic algorithms. *Scientific American*, *267*(1), 66–72.

Holzer, D., Hough, R., & Burr, M. (2007). Parametric design and structural optimisation for early design exploration. *International Journal of Architectural Computing*, *5*(4), 625–643. https://doi.org/10.1260/147807707783600780

Jaspart, J.-P., & Weynand, K. (2017). *Design of joints in steel structures - eurocode 3 - design of steel structures - part 1-8 - design of joints (uk edition)*. John Wiley & Sons.

Kabanda, J. S., & MacDougall. (2017). Comparison of the moment rotation capacities of rectangular and polygonal hollow sections. *Journal of Constructional Steel Research*, *137*, 66–76. https://doi.org/https://doi.org/10.1016/j.jcsr.2017.06.005

Kaethner, S. C., & Burridge, J. A. (2012). Embodied co2 of structural frames. *TheStructuralEngineer*, *90*(5), 33–40.

Kirsch, U. (1993). *Structural optimization : Fundamentals and applications*. Springer.
Kramer, O. (2017). *Genetic algorithm essentials*. springer.
Makert, R., & Alves, G. (2016). Between designer and design: Parametric design and prototyping considerations on gaudí's sagrada familia. *Periodica Polytechnica Architecture*, *47*(2), 89–93.
Martin, L. H., & Purkiss, J. A. (2007). *Structural design of steelwork to en 1993 and en 1994* (3rd ed.). Elsevier.
Momber, A. (2008). *Blast cleaning technology*. Springer.
Pipinato, A. (2021). *Innovative bridge design handbook - construction, rehabilitation and maintenance* (2nd ed.). Elsevier.
Rothlauf, F. (2006). *Representations for genetic and evolutionary algorithms*. Springer.
Sivanandam, S., & Deepa, S. (2008). *Introduction to genetic algorithms*. Springer.
Soutsos, M., & Domone, P. (n.d.). *Construction materials: Their nature and behaviour* (5th ed.). CRC Press.
Trvk bro 11. (2011). Trafikverket.
UN, U. N. E. P. (2021). *2021 global status report for buildings and construction: Towards a zero-emission, efficient and resilient buildings and construction sector*.
Whitehead, R. (2019). *Structures by design : Thinking, making, breaking*. Taylor & Francis Group.
Yang, X.-S. (2010). *Engineering optimization : An introduction with metaheuristic applications*. John Wiley & Son.
Yang, X.-S. (2014). *Nature-inspired optimization algorithms*. Elsevier.

A

Cross-sections

VKR-HÅLPROFILER

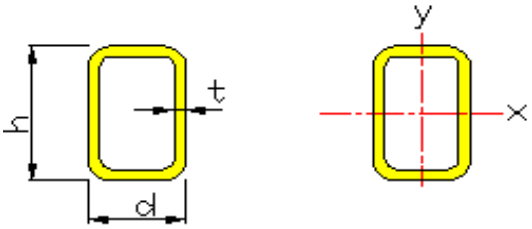

Storhetsbeteckningar
g = Massa per m
F = Mantelyta per m
A = Tvärsnittsarea
$I_{x, y}$ = Yttröghetsmoment
$W_{x, y}$ = Elastiskt böjmotstånd
$Z_{x, y}$ = Plastiskt böjmotstånd
$i_{x, y}$ = Tröghetsradie
K_v = Vridstyvhetens tvärsnittsfaktor
W_v = Elastiskt vridmotstånd

Stålsort: S355J2H

Dimension	Vikt och ytor			Böjning i x-led				Böjning i y-led				Vridning	
	g	F	A	I_x	W_x	Z_x	i_x	Iy	Wy	Zy	iy	K_v	W_v
	kg/m	m²/m	mm²	mm⁴	mm³	mm³	mm	mm⁴	mm³	mm³	mm	mm⁴	mm³
				*10⁶	*10³	*10³		*10⁶	*10³	*10³		*10⁶	*10³
50*50*5.0	6.85	0.187	873	0.289	11.6	14.5	18.2	0.289	11.6	14.5	18.2	0.476	16.7
60*60*5.0	8.42	0.227	1070	0.533	17.8	21.9	22.3	0.533	17.8	21.9	22.3	0.864	25.7
70*70*5.0	9.99	0.267	1270	0.885	25.3	30.8	26.4	0.885	25.3	30.8	26.4	1.42	36.8
80*80*5.0	11.6	0.307	1470	1.37	34.2	41.1	30.5	1.37	34.2	41.1	30.5	2.17	49.8
90*90*5.0	13.1	0.347	1670	2.00	44.4	53.0	34.5	2.00	44.4	53.0	34.5	3.16	64.8
100*100*4.0	11.9	0.390	1520	2.32	46.4	54.4	39.1	2.32	46.4	54.4	39.1	3.61	68.2
100*100*5.0	14.7	0.387	1870	2.79	55.9	66.4	38.6	2.79	55.9	66.4	38.6	4.39	81.8
100*100*6.0	17.4	0.385	2220	3.23	64.6	77.6	38.2	3.23	64.6	77.6	38.2	5.13	94.3
100*100*8.0	22.6	0.379	2880	4.00	79.9	98.2	37.3	4.00	79.9	98.2	37.3	6.46	116
100*100*10.0	27.4	0.374	3490	4.62	92.4	116	36.4	4.62	92.4	116.0	36.4	7.61	133
120*120*5.0	17.8	0.467	2270	4.98	83.0	97.6	46.8	4.98	83.0	97.6	46.8	7.77	122
120*120*6.0	21.2	0.465	2700	5.79	96.6	115	46.3	5.79	96.6	115.0	46.3	9.11	141
120*120*8.0	27.6	0.459	3520	7.26	121	146	45.5	7.26	121.0	146.0	45.5	11.60	176
120*120*10.0	33.7	0.454	4290	8.52	142	175	44.6	8.52	142	175	44.6	13.82	206
140*140*5.0	21.0	0.547	2670	8.07	115	135	55.0	8.07	115	135	55.0	12.53	170
140*140*6.0	24.9	0.545	3180	9.44	135	159	54.5	9.44	135	159	54.5	14.75	198
140*140*8.0	32.6	0.539	4160	11.95	171	204	53.6	11.95	171	204	53.6	18.92	249
140*140*10.0	40.0	0.534	5090	14.16	202	246	52.7	14.16	202	246	52.7	22.72	294
140*140*12.5	48.7	0.528	6210	16.53	236	293	51.6	16.53	236	293	51.6	26.96	342
150*150*5.0	22.6	0.587	2870	10.02	134	156	59.0	10.02	134	156	59.0	15.50	197
150*150*6.0	26.8	0.585	3420	11.74	156	184	58.6	11.74	156	184	58.6	18.28	230
150*150*8.0	35.1	0.579	4480	14.91	199	237	57.7	14.91	199	237	57.7	23.51	291
150*150*10.0	43.1	0.574	5490	17.73	236	286	56.8	17.73	236	286	56.8	28.32	344
150*150*12.5	52.7	0.568	6710	20.80	277	342	55.7	20.80	277	342	55.7	33.75	402
160*160*6.0	28.7	0.625	3660	14.37	180	210	62.7	14.37	180	210	62.7	22.33	264
160*160*8.0	37.6	0.619	4800	18.31	229	272	61.8	18.31	229	272	61.8	28.80	335
160*160*10.0	46.3	0.614	5890	21.86	173	329	60.9	21.86	173	329	60.9	34.78	398
160*160*12.5	56.6	0.608	7210	25.76	322	395	59.8	25.76	322	395	59.8	41.58	467
180*180*6.0	32.5	0.705	4140	20.77	231	269	70.9	20.77	231	269	70.9	32.15	340
180*180*8.0	42.7	0.699	5440	26.61	296	349	70.0	26.61	296	349	70.0	41.62	434
180*180*10.0	52.5	0.694	6690	31.93	355	424	69.1	31.93	355	424	69.1	50.48	518
180*180*12.5	64.4	0.688	8210	37.90	421	511	68.0	37.90	421	511	68.0	60.70	613
200*200*6.0	36.2	0.785	4620	28.83	288	335	79.0	28.83	288	335	79.0	44.49	426
200*200*8.0	47.7	0.779	6080	37.09	371	436	78.1	37.09	371	436	78.1	57.78	545
200*200*10.0	58.8	0.774	7490	44.71	447	531	77.2	44.71	447	531	77.2	70.31	655
200*200*12.5	72.3	0.768	9210	53.36	534	643	76.1	53.36	534	643	76.1	84.91	778
200*200*16.0	90.3	0.759	11500	63.94	639	785	74.6	63.94	639	785	74.6	103.40	927
220*220*6	40.0	0,859	5043	38.75	352	408	87.2	38.75	352	408	87.2	59.63	521
220*220*10	65.1	0,837	8057	60.50	550	650	85.4	60.50	550	650	85.4	94.73	807
250*250*6.0	45.7	0.985	5820	57.52	460	531	99.4	57.52	460	531	99.4	88.25	681

250*250*8.0	60.3	0.979	7680	74.55	596	694	98.6	74.55	596	694	98.6	115.25	880
250*250*10.0	74.5	0.974	9490	90.55	724	851	97.7	90.55	724	851	97.7	141.06	1065
250*250*12.5	91.9	0.968	11700	109.15	873	1037	96.6	109.15	873	1037	96.6	171.64	1279
80*40*5.0	8.42	0.227	1070	0.803	20.10	26.10	2.74	0.257	12.9	15.7	1.55	0.651	21.9
90*50*5.0	9.99	0.267	1270	1.27	28.2	36.0	31.6	0.492	19.7	23.5	19.7	1.16	32.9
100*50*5.0	10.8	0.287	1370	1.67	33.4	42.6	34.9	0.543	21.7	25.8	19.9	1.35	36.9
100*60*5.0	11.6	0.307	1470	1.89	37.8	47.4	35.9	0.836	27.9	32.9	23.8	1.88	45.9
120*60*4.0	10.7	0.350	1360	2.49	41.5	51.9	42.8	0.931	31.0	31.7	26.2	2.01	47.1
120*60*5.0	13.1	0.347	1670	2.99	49.8	63.1	42.3	0.988	32.9	38.4	24.3	2.42	26.0
120*60*6.0	15.5	0.345	1980	3.45	57.5	73.6	41.7	1.13	37.7	44.5	23.9	2.79	63.8
120*60*6.3	16.2	0.344	2070	3.58	59.7	76.7	41.6	1.16	38.7	46.3	23.7	2.90	65.9
120*60*8.0	20.1	0.339	2560	4.25	70.8	92.7	40.7	1.35	45.0	55.4	23.0	3.44	76.6
120*80*4.0	11.9	0.390	1520	3.03	50.5	61.2	44.6	1.61	40.3	46.1	32.5	3.30	65.0
120*80*5.0	14.7	0.387	1870	3.65	60.8	74.6	44.2	1.93	48.3	56.1	32.1	4.01	77.9
120*80*6.0	17.4	0.384	2220	4.23	70.5	87.3	43.7	2.22	55.5	65.5	31.6	4.68	89.6
120*80*8.0	22.6	0.379	2880	5.25	87.5	111	42.7	2.73	68.3	82.6	30.8	5.87	110
120*80*10.0	27.4	0.374	3490	6.09	101.5	131	41.8	3.13	78.3	97.3	29.9	6.88	126
140*70*4.0	12.6	0.410	1600	4.04	57.7	71.7	50.2	1.36	38.8	44.0	29.1	3.25	66.0
140*70*5.0	15.5	0.417	1970	4.88	59.8	87.6	49.8	1.63	46.5	53.5	28.7	3.94	79.0
140*70*6.3	19.2	0.404	2440	5.89	84.2	107	49.1	1.94	55.3	65.0	28.1	4.77	94.0
140*80*4.0	13.2	0.430	1680	4.41	62.9	77.1	51.2	1.84	46.0	52.2	33.1	4.11	76.5
140*80*6.3	20.2	0.424	2570	6.46	92.3	115	50.1	2.65	66.2	77.5	32.1	6.07	110
150*100*4.0	15.1	0.490	1920	6.07	80.9	97.4	56.2	3.24	64.8	73.6	41.1	6.60	105
150*100*5.0	18.6	0.487	2370	7.39	98.5	119	55.8	3.92	78.4	90.1	40.7	8.07	127
150*100*6.0	22.1	0.485	2820	8.62	114.9	141	55.3	4.56	91.2	106	40.2	9.46	147
150*100*8.0	28.9	0.479	3680	10.87	144.9	180	54.3	5.69	113.8	135	39.3	12.03	183
150*100*10.0	35.3	0.474	4490	12.82	170.9	216	53.4	6.65	133.0	161	38.5	14.32	214
160*80*4.0	14.4	0.470	1840	6.12	76.5	94.7	57.7	2.07	51.8	58.3	33.5	4.93	88.1
160*80*5.0	17.8	0.467	2270	7.44	93.0	116	57.2	2.49	62.3	71.1	33.1	6.00	106
160*80*6.0	21.2	0.465	2700	8.68	108.5	136	56.7	2.88	72.0	83.3	32.7	7.01	122
160*80*10.0	33.7	0.454	4290	12.84	160.5	209	54.7	4.11	103	125	31.0	10.41	175
160*90*5.0	18.6	0.487	2370	8.04	101.0	124	58.2	3.26	72.5	82.7	37.1	7.38	121
160*90*8.0	28.9	0.482	3680	11.80	148.0	187	56.8	4.70	105	124	35.8	11.00	174
180*100*6.0	24.9	0.545	3180	13.60	151.1	186	65.4	5.36	107	123	41.1	12.24	179
180*100*8.0	32.6	0.539	4160	17.13	190.3	239	64.2	6.71	134	157	40.2	15.60	224
180*100*10.0	40.0	0.534	4540	18.47	205.2	259	63.8	7.20	144	170	39.8	16.85	240
200*100*5.0	22.6	0.587	3870	14.95	149.5	185	62.2	5.05	101	114	36.1	12.04	172
200*100*6.0	26.8	0.585	3420	17.54	175.4	218	71.6	5.89	118	134	41.5	14.14	200
200*100*8.0	35.1	0.579	4480	22.34	223.4	282	70.6	7.39	148	172	40.6	18.04	251
200*100*10.0	43.1	0.574	5490	26.64	266.4	341	69.7	8.69	174	206	39.8	21.56	295
200*100*12.5	52.7	0.568	6710	31.36	313.6	408	68.4	10.04	201	245	38.7	25.41	341
200*120*6.0	28.7	0.625	3660	19.80	198.0	242	73.6	8.92	149	169	49.4	19.42	245
200*120*8.0	37.6	0.619	4800	25.29	252.9	313	72.6	11.28	188	218	48.5	24.95	310
200*120*10.0	46.3	0.614	5890	30.26	302.6	379	71.7	13.37	223	263	47.6	30.01	367
220*120*6	30.6	0,656	3897	25.00	227.3	280	80.1	9.70	162	183	49.9	22.17	271
220*120*8.0	40.2	0.659	5120	32.00	290.9	362	79.1	12.30	205	236	49.0	28.50	343
220*120*10.0	49.4	0.656	6290	38.40	349.0	440	78.2	14.60	243	285	48.1	34.30	407
250*150*6.0	36.2	0.785	4620	39.65	317.2	385	92.6	17.96	239	270	62.3	38.77	396
250*150*8.0	47.7	0.779	6080	51.11	408.9	501	91.7	22.98	306	350	61.5	50.21	56
250*150*10.0	58.8	0.774	7490	61.74	493.9	611	90.8	27.55	367	426	60.6	60.90	605
250*150*12.5	72.3	0.768	9210	73.87	591.0	740	89.6	32.65	435	514	59.5	73.26	717
260*140*6.0	36.2	0.785	4620	41.68	321	393	95.0	15.91	227	255	58.7	36.38	383
260*140*8.0	47.7	0.779	6080	53.73	413	511	94.0	20.32	290	331	57.8	47.04	488

B

Appendix 2

Bridge Number
100-63-1
100-67-1
15-1795-1
100-219-1
16-845-2
3501-9001-1
22-1603-1
100-217-1
15-1582-1
100-92-1
2-2183-1
2-2152-1
3-819-1
2-83-2
17-1277-1
3501-6223-1
13-969-1
14-1651-1
14-1607-1
12-1301-1
3501-6206-1
3501-6226-1
21-1186-1
3501-5973-1
22-1169-1
2-1908-1
3501-5501-1
22-1136-1
12-1031-1
20-966-1
6-898-1
24-1462-1
20-1363-1
21-798-1
17-930-1
3501-5670-1